Influence of an Individualised Shoulder Belt Position for Diverse Occupant Anthropometries on Seatbelt Interaction in Frontal and Side Impacts

Influence of an Individualised Shoulder Belt Position for Diverse Occupant Anthropometries on Seatbelt Interaction in Frontal and Side Impacts

Alexandros Leledakis, Jonas Östh, Johan Iraeus, Johan Davidsson, Lotta Jakobsson

Abstract This simulation study investigated the influence of individualised shoulder belt position on seatbelt interaction and occupant kinematics in two frontal and one far side impact, considering the variability of occupant anthropometry and sitting postures. Morphed Human Body Models, positioned as front passengers, were simulated in 132 setups. For every occupant, an individualised shoulder belt position configuration was created by changing the D-ring mounting location, aiming for a mid-shoulder belt fit. A *"traditional belt"* configuration was also tested, with the D-ring mounted on the B-pillar. The initial belt's placement over the occupant's shoulder was influential; however, it may not necessarily lead to an overall improved seatbelt interaction as a single parameter. Different occupants were associated with different seatbelt interaction challenges. Tall occupants with low Body Mass Index (BMI) were more likely to slide out of the shoulder belt, while short low-BMI occupants were more likely to submarine. The early torso to pelvis retention balance and the torso's axial rotations were identified as the main mechanisms behind those observations. The study identified seatbelt interaction challenges for different occupant groups and could facilitate the analysis of additional changes in belt characteristics towards individualised occupant restraint systems.

Keywords Anthropometric Variation, Human Body Model, Individualised Restraint Systems, Morphing.

I. INTRODUCTION

The seatbelt is one of the most important components of occupant restraint systems in contemporary cars. For the belt to function effectively, it should be placed over the strong load-bearing bones of the occupant, such as the pelvic bone, sternum and clavicle. Additionally, restraining the pelvis while allowing a controlled "*forward-pitching*" motion of the torso is desirable to avoid interaction between the lap belt and the sensitive abdominal region, so-called submarining [1]. It is generally accepted that a mid-shoulder belt placement is considered to be optimal [1–4]. A shoulder belt positioned on the lateral part of the shoulder could increase the likelihood of the occupant's torso sliding out of the shoulder belt. On the other hand, placing the shoulder belt close to the neck could be associated with discomfort, which could even lead occupants to misplace the shoulder belt [2].

Moreover, belt fit can depend on the occupant's characteristics, such as stature, Body Mass Index (BMI), sex, and age [5-6], as well as the occupant's posture [7]. For subjects with high BMI, the lap belt is typically further forward and higher, relative to the Anterior Superior Iliac Spine (ASIS) [6], and the shoulder belt is laterally towards the buckle side and higher on the ribcage [8]. The shoulder belt fit, quantified by the lateral location of the shoulder belt relative to the torso centreline at the height of the suprasternale, is also strongly affected by the location of the seatbelt's anchorage points [6]. Additionally, in certain anchorage locations, differences between females and males were observed in terms of an increased gap between the shoulder belt and the sternum [6].

Recent studies have used morphed Human Body Models (HBMs) to investigate the influence of occupant anthropometric variability [9-10] during a vehicle impact and to develop methods for supporting the design of restraint systems that can accommodate such variability [11–15]. Aspects, such as restraint characteristics and lap belt fit, have – to some extent – been investigated. However, studies investigating the influence of shoulder belt routing during impact have mainly targeted child occupants [16-17], leaving a research gap about adults.

The sensitivity of belt fit to anthropometric variations and relative position to anchorage points calls for the investigation of the effect of initial shoulder belt fit on occupant responses during an impact. As a step towards enhancing the understanding of individualised occupant restraint systems, that would be tailored to the characteristics of the occupant using them, the objective of this study was to investigate the influence of an individualised shoulder belt position on seatbelt interaction and occupant kinematics, considering the variability of occupant anthropometry, seat positions and sitting postures.

A. Leledakis (alexandros.leledakis@chalmers.se, +46 72 885 2398) is an Industrial PhD student at Chalmers University of Technology and Volvo Cars, Gothenburg, Sweden. J. Östh, PhD, is a Technical Expert for Human Body Modelling and L. Jakobsson, PhD, a Senior Technical Leader in Injury Prevention at the Volvo Cars Safety Centre, Gothenburg, Sweden. J. Iraeus, PhD, is a Senior Researcher, J. Davidsson, PhD, an Associate Professor, L. Jakobsson an Adjunct Professor, and J. Östh an Adjunct Associate Professor at Chalmers University of Technology, Gothenburg, Sweden. All authors are associated with SAFER – Vehicle and Traffic Safety Centre at Chalmers in Sweden.

II. METHODS

A Finite Element (FE) simulation study was conducted, utilising morphed HBMs, positioned as front passengers in 132 setups. The setups included: 22 HBMs of varying shape, size, and sex, three occupant sitting postures, and two seat fore-aft positions. For every occupant, an Individualised Shoulder Belt Position (ISBP) configuration was created by changing the D-ring mounting location, aiming for a mid-shoulder belt fit. A *"traditional belt" configuration* was also tested, with the D-ring mounted on the B-pillar (at the same position for all occupants). The HBMs were subjected to three crash pulses for all setups, leading to a total of 792 in-crash simulations. The included parameters are illustrated in Fig. 1.

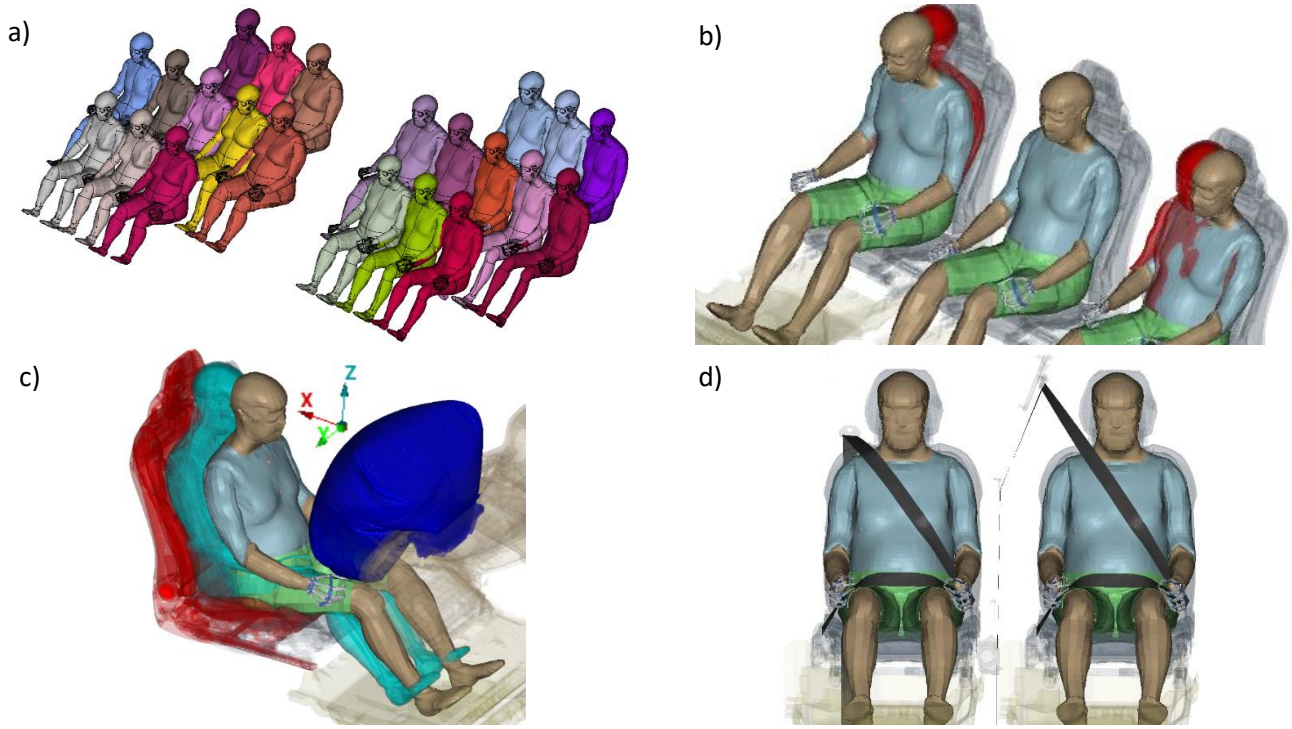

Fig. 1. Overview of the included parameters: (a) the 11 female and male HBM sizes, (b) the occupant postures, including the forward-leaning and inboard-leaning occupant postures (with the nominal posture overlaid in red and in the middle), (c) the simulation environment, with the occupant seated in the two seat fore-aft positions, and (d) the Individualised Shoulder Belt Position (ISBP) and traditional belt configurations.

Vehicle Interior and Occupant Surrogates

To model the car occupant, 22 occupant anthropometries, comprising 11 HBMs with male body shapes and 11 HBMs with female body shapes, were morphed from the SAFER HBM v9.0.1 [18]. The female cohort had a nominal height of 162 cm with a range of 148 cm to 176 cm, while the male cohort showed a nominal height of 176 cm with a range of 162 cm to 190 cm. Besides nominal-BMI occupants (28 kg/m^2), the BMI varied in the range of 18 to 38 kg/m^2, covering underweight (18 kg/m^2) and obese (38 kg/m^2) occupants, respectively. The occupant's age was kept constant at 40 years old.

The baseline HBM represents a 50th percentile male with a stature of 175 cm and a weight of 77 kg. Its biofidelity has been assessed in frontal, near- and far- side impacts [19–23]. In a previous study [24], the baseline HBM was morphed [21][25] utilising statistical models of the body surface, pelvis, femur, tibia and ribcage. Morphed models of the SAFER HBM v9 have been evaluated in side impacts and have shown improved kinematics prediction compared with the baseline model [21][26].

A deformable vehicle interior with approximately 2.35 million Finite Elements (FE) contained in a rigid body-in-white, previously validated [27], was used to model the interior of a mid-sized SUV. The simulations were conducted using the explicit FE solver LS-DYNA MPP s R9.3.0 (ANSYS/LST, Livermore, CA, USA) on the same cluster (using 140 CPUs) to eliminate variation due to model decomposition [28]. A right-handed coordinate system (Fig. 1) was used, defined with X rearward, Z upward, and Y toward the vehicle's right side.

Seat Adjustments and Occupant Postures

A mid- and a rearward- seat position, located at 40% and 100% of the fore-aft travel, respectively, were used. These positions were selected to encompass the fore-aft seat adjustments observed in approximately 95% of

travel time during a naturalistic driving study involving 75 vehicles [29]. Additionally, the seat backrest was always adjusted in an upright position of 25°. The three occupant postures included the nominal posture (upright, centred in the seat, looking in the direction of travel with feet on the footrest) as well as two additional postures [27], with the occupant leaning inboard (approximately 7°) as if the car was turning [30] and leaning forward (approximately 8°) as if the car was decelerating [27] (Fig. 1).

To ensure consistency, an automated method [24] was used to position the HBMs in all seat positions and postures, utilising the marionette method [31].

Occupant Restraint Systems

The restraint system used in the simulations included a model of a pyrotechnically-pretensioned three-point seatbelt that was load-limited (to 4.2 kN at 180 mm of belt payout) and a frontal passenger airbag that deployed upwards from the dashboard (Fig. 1). The load-limiter was selected to be within the range, indicated by [32], encompassing subcompact to SUV cars manufactured between 2003 to 2010 and sold in the European market. The activation timing of the restraint systems was kept constant for all occupant sizes, postures, seat positions, and seatbelt configurations.

To achieve the individualised shoulder belt position, the D-ring position was adjusted in relation to the midpoint of the HBM's clavicle. The D-ring was kept at a constant distance from the clavicle of 300 mm and an angle of 35° relative to the sagittal plane and 10° relative to the transverse plane (Appendix A, Fig. A.1-3). The angles were chosen with the goal of placing the shoulder belt over the occupant's mid-shoulder, regardless of the occupant's size (Appendix B). The D-ring position was set with the occupant in the nominal posture and was not adjusted when the posture was changed, although it was adjusted to follow the seat's position. In both configurations, the lap belt anchor and buckle were fixed to the seat and moved with it when the seat was moved.

In all setups, the belt was routed over the positioned HBMs utilising the shortest path algorithm, to minimise slack, using the Primer v18 software (Oasys Ltd, Solihull, United Kingdom).

Crash Configurations

The occupants were exposed to crash pulses originating from three crash configurations (Fig. 2). A high-severity Oncoming Frontal impact [24] was simulated, featuring approximately 50% overlap and an initial velocity of 50kph for both vehicles. Additionally, two crash configurations, identified in [33] as representative of potential future intersection crashes were simulated: an Intersection Frontal impact with approximately 50% overlap of the left front, and a Far-Side impact to the front left corner. The intersection crash configurations were relatively low-severity impacts. Crash pulses were generated from car-to-car impact simulations as described in [24][27]. The HBM in-crash simulations were carried out by applying the motion from the car-to-car impacts to the vehicle's interior model using prescribed rigid-body six-degrees-of-freedom translational and rotational velocities. The frontal and the Far-Side impacts were simulated for 200 ms and 300 ms, respectively.

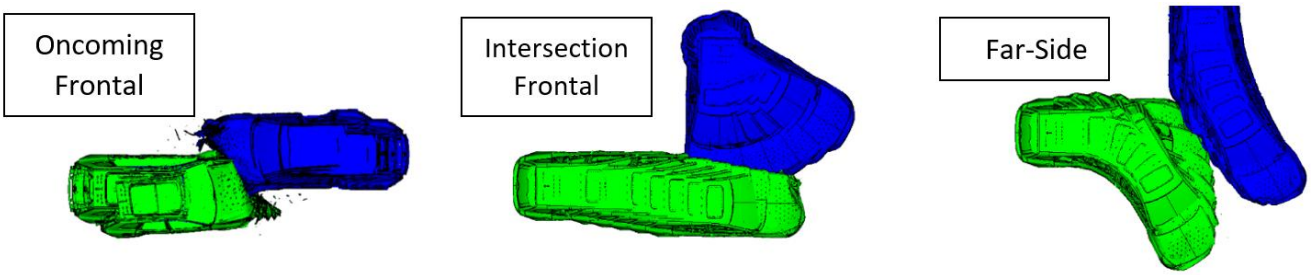

Fig. 2. Vehicle motion of the crash configurations. During the crash simulations, the HBM was in the front, Right-Hand Side (RHS), passenger seat of the green vehicle.

Analysis Methods

To identify patterns in the occupant's kinematic responses and seatbelt interaction across all parameters, a Global Sensitivity Analysis (GSA) method [24], coupled with a full-factorial Design of Experiment (DOE), was used. The GSA employed one-at-time comparisons, where the investigated parameter was varied while all others were held constant. The sensitivity metric comprised the median and the interquartile range (IQR) (25^{th} to 75^{th} percentile)

of the relevant comparisons. The median value represented the parameter's main effect, while the IQR indicated the presence of interaction effects.

The analysis focused on the time interval up to 20 ms after the rebound onset for each simulation, hereafter called "*full-sequence*". The start of the rebound phase (rebound onset) was calculated as the time when the occupant's torso and pelvis velocity relative to the car changed sign in the longitudinal or lateral direction for the frontal and side impacts, respectively. Two additional time intervals facilitated the analysis of the occupant responses, the $t_{0\rightarrow R\text{-}10}$ and $t_{R\text{-}10\rightarrow R+20}$. The $t_{0\rightarrow R\text{-}10}$ spanned from the start of the impact up to 10 ms prior to the rebound onset. The $t_{R\text{-}10\rightarrow R+20}$ was defined as starting 10 ms prior to the rebound onset and ending 20 ms post the rebound onset. Furthermore, for the frontal impact simulations, if submarining was detected, the analysis time interval was reduced to exclude data after the submarining occurrence from further analysis.

The kinematic responses were evaluated based on the excursion (in the X- and Y- directions) of selected anatomical landmarks relative to the vehicle. Torso angles were also tracked, with the torso angle defined in the XZ (pitch) and YZ (roll) planes using the sacrum and T8 vertebra, while the axial (around Z-axis) rotation was calculated using the left and right acromion in the YZ plane. Additionally, for the frontal impacts, the ratio of Torso to Pelvis excursion (TtPe) was calculated, at 60 ms, using the sternum (middle of gladiolus, at the fourth rib height) and the pelvis Centre of Gravity (CoG), as a metric of shoulder to lap belt retention balance.

The seatbelt interaction was quantified, in terms of the belt's position on the occupant, by measuring the distance of the belt relative to occupants' anatomical landmarks. Euclidean planes were constructed using three anatomical landmarks of the pelvis, thoracic cage and clavicle (Appendix B). The motion of the belt in those planes was measured relative to the anatomical landmark of interest prior to the impact, for the initial belt fit, and over time, for the belt interaction. For the lap belt, the left and right ASIS were used. For the shoulder belt, the HBM's sternum and the distal end of the right clavicle were used.

To produce a shoulder belt placement metric, comparable across occupants of different shapes and sizes, the placement of the inner belt edge relative to the clavicle was normalised with the length of the clavicle, resulting in the creation of the Shoulder Belt Clavicle Placement (SBCP) metric (Fig. 3). The SBCP scale was defined with 0% corresponding to the inner edge of the shoulder belt being positioned over the proximal end of the clavicle, and 100% corresponding to the inner edge of the shoulder belt being positioned over the distal end of the clavicle. To characterise the initial belt fit, the midpoint of the shoulder belt on the sternum and clavicle was used to define the Shoulder Belt Clavicle Placement midpoint (SBCPm) metric in a similar manner.

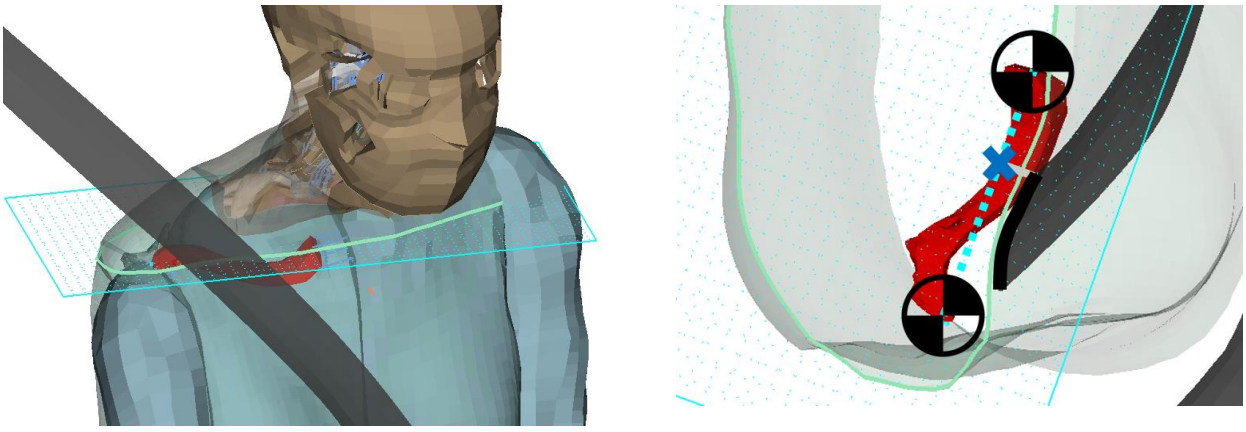

Fig. 3. Illustration of the shoulder belt positioned over the occupant's shoulder in the plane of the clavicle. The SBCP (inner edge of the shoulder belt placed along the length of the clavicle) was at 35%, in this example.

To identify potentially critical belt interaction events, the placement of the belt relative to the occupant was analysed. Specifically, the longitudinal placement of the lap belt's upper edge, relative to the ASIS, was used to detect submarining events. The severity grading of these events was determined based on timing (Table I).

TABLE I
LAP BELT TO ASIS INTERACTION CLASSIFICATION

Classification	*Value*	*Interpretation*
Lap belt stays in front of ASIS	P0	The upper edge of the lap belt was never positioned closer than 10 mm in the longitudinal direction to either of the ASIS, in the full-sequence time interval
Marginal submarining on at least one side	P1	The upper edge of the lap belt was positioned closer than 10 mm in the longitudinal direction for at least one of the ASIS, in the $t_{R-10 \rightarrow R+20}$ time interval
Submarining on one side	P2	The upper edge of the lap belt was positioned behind the ASIS on one side, in the $t_{0 \rightarrow R-10}$ time interval
Submarining on both sides	P3	The upper edge of the lap belt was positioned behind the ASIS on both sides, in the $t_{0 \rightarrow R-10}$ time interval

Similarly, the lateral placement of the shoulder belt's inner edge, along the clavicle, was used to detect events such as "*belt close to the neck*" or "*shoulder sliding out of the belt*", as detailed in Table II.

TABLE II
SHOULDER BELT TO CLAVICLE INTERACTION CLASSIFICATION

Classification	*Value*	*Interpretation*
Belt close to the neck	S-1	The inner edge of the shoulder belt did not go beyond 10% SBCP, in the full-sequence time interval
Shoulder belt remains on the shoulder	S0	The inner edge of the shoulder belt remained below 85% SBCP, in the full-sequence time interval
Shoulder belt close to the distal clavicle end	S1	The inner edge of the shoulder belt moved past the 85% SBCP, in the full-sequence time interval
Shoulder slides out of the belt late	S2	The inner edge of the shoulder belt moved past the 100% SBCP (distal end of the clavicle), in the $t_{R-10 \rightarrow R+20}$ time interval
Shoulder slides out of the belt	S3	The inner edge of the shoulder belt moved past the 100% SBCP (distal end of the clavicle), in the $t_{0 \rightarrow R-10}$ time interval

III. RESULTS

Out of the 792 simulations, 789 simulations reached normal termination. The three simulations that terminated too early, were frontal impact simulations in which submarining was observed, and they were terminated when the occupant was already in the rebound phase (earliest at 130 ms). Despite these error terminations, the failed simulations provided sufficient data for further analysis.

The following subsections present the most important results related to initial belt fit and occupant kinematics and belt motion relative to the shoulder and pelvis in the simulated 1) Oncoming Frontal, 2) Intersection Frontal, and 3) Far-Side impacts. More detailed information can be found in Appendices C – E.

Initial Belt Fit

The occupant's initial shoulder belt fit was influenced by all parameters varied in this simulation study (BMI, stature, sex, seat position, and occupant's posture), as exemplified in Fig. 4. Overall, the shoulder belt was positioned closer to the neck of the occupant with the traditional belt configuration (SBCPm median: 21%, IQR: 37%) compared to the ISBP belt configuration (SBCPm median: 34%, IQR: 16%). The lower IQR of the ISBP belt configuration indicated that the shoulder placement of the belt was less influenced by the varied parameters compared to the traditional belt configuration.

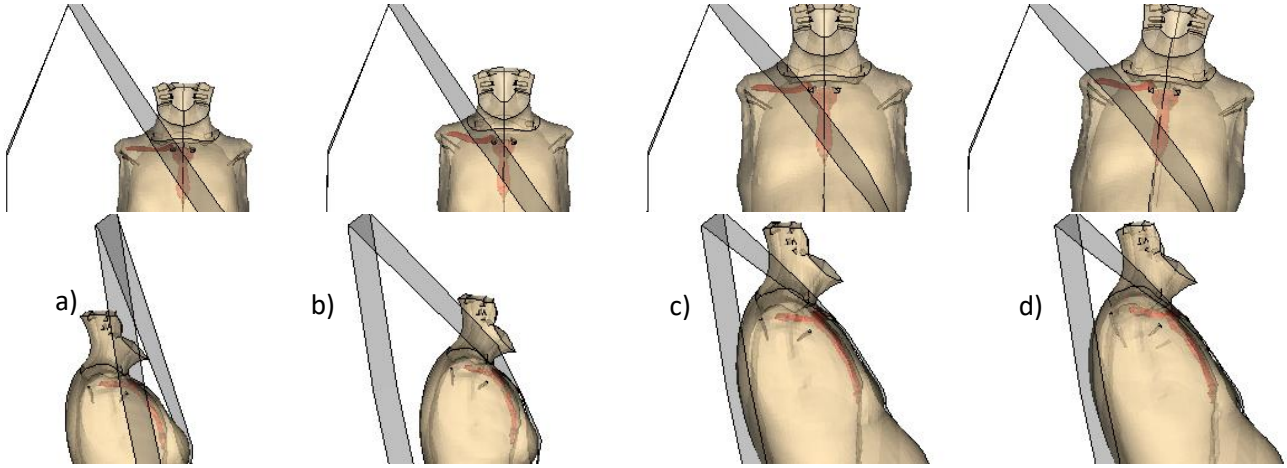

Fig. 4. Belt fit examples: a) F – 148 cm – 23 kg/m^2 – Nominal posture – rearward seat, the belt is at 1% SBCP with 52 mm of gap; b) F – 148 cm – 23 kg/m^2 – Leaning forward posture – mid seat, the belt is at 11% SBCP with no gap; c) M – 176 cm – 33 kg/m^2 – Nominal posture – mid seat, the belt is at 29% SBCP with no gap; and d) M – 176 cm – 33 kg/m^2 – Leaning inboard posture – mid seat, the belt is at 76% SBCP with no gap.

Irrespective of the seat belt configuration, occupants with higher than nominal BMI tended to have the shoulder belt placed more laterally, towards the left-hand side (LHS), at the mid-sternum height, and more proximal, towards their neck, at clavicle height. Moreover, it was found that with the traditional belt configuration, the position of the seat had an impact on the longitudinal placement (gap) of the shoulder belt on the clavicle. The occurrence of this gap was more frequent for occupants with a stature below the nominal and BMI above the nominal, and was increased in rearward-positioned seats. However, when the occupants leaned forward, the gap was reduced by an average of 24 mm. More detailed information about the initial belt position, for both belt configurations, can be found in Appendix C.

Oncoming Frontal

In the Oncoming Frontal impact simulations, the lap belt stayed in front of the ASIS (P0 or P1 classification in Table I) when using the traditional belt configuration. However, with the ISBP belt configuration and occupants in the nominal posture, submarining (P2 and P3 classification, Table I) events were observed for 6 out of the 22 occupants, in the mid-positioned seat, and for 12 out of 22 in the rearward-positioned seat (Fig. 5). As seen in Fig. 5, occupants at the lower end of the BMI and stature scales, were more likely to submarine. The lap belt interaction classification, for all belt configurations, seat positions and occupant postures can be seen in Appendix D.

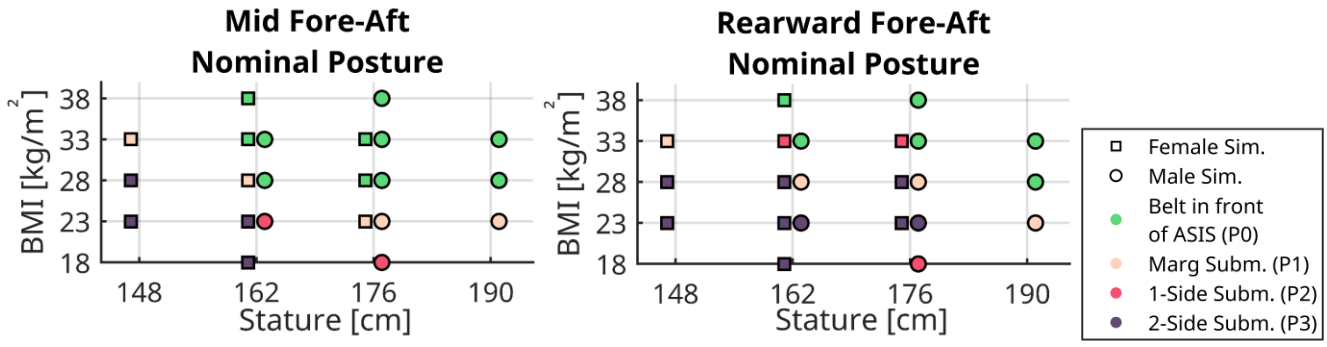

Fig. 5. Lap belt to ASIS interaction classification during Oncoming Frontal simulations with ISBP belt configuration for occupants in nominal posture and seated in mid- (left) and rearward- (right) positions.

Two mechanisms were identified, the TtPe ratio, which was associated with the occurrence of submarining and the torso axial rotation, which was associated with sliding out of the shoulder belt events. These mechanisms are presented at the 60th ms of the impact, before the earliest observation of submarining among all setups. Thereafter, for the subgroup of simulations, in which no submarining was observed, analysis was performed in the full-sequence time interval to analyse shoulder belt interaction.

Torso to Pelvis excursion (TtPe)

With the traditional belt configuration, the median TtPe was 0.9 at the 60th ms of the impact, in all tested setups, indicating that for every 100 mm of pelvis excursion, the torso had a median excursion of 90 mm. The most influential parameters are reported below.

- *BMI:* A strong influence of BMI on TtPe was observed (Fig. 6). Underweight occupants had a larger TtPe compared to obese occupants (Fig. 7). Compared to nominal-BMI occupants, underweight occupants had a median increase of 0.26, and obese occupants had a reduction of 0.06. Interaction effects with seat position and occupant posture were also found (Fig. 6). The influence of BMI was amplified in the rearward-position seat (underweight +0.39, obese -0.08) and reduced when the seat was in the mid-position (underweight +0.23, obese 0) or when the occupant was leaning forward (underweight +0.19, obese 0).
- *Seat position*: With the seat in the rearward-position, the median TtPe increased by 0.13, compared to when the seat was in the mid-position. The interaction effect observed between seat position and BMI (Fig. 6) was attributed to two factors. Firstly, underweight occupants exhibited increased torso excursions (+28 mm, +32%) when the seat was in the rearward-position, compared to the mid-position. A smaller increase in torso excursions was seen for obese occupants (+14 mm, +12%). Secondly, an increase in pelvic excursions was observed for obese occupants (10 mm), which was not seen for other BMI groups.
- *Posture:* Compared to occupants in the nominal posture, a median reduction of 0.14 in TtPe was seen when the occupants were leaning forward before the impact. The driving factor for the influence of posture was the reduced torso excursions, as the pelvis excursions were essentially unaffected by the initial posture.
- *Stature:* No clear trends were generally seen between stature and TtPe. However, for tall occupants (190 cm), an increase of 0.27 was seen when they were positioned in the mid-position seat, as their knees came into contact with the dashboard earlier, limiting their pelvis' excursion.

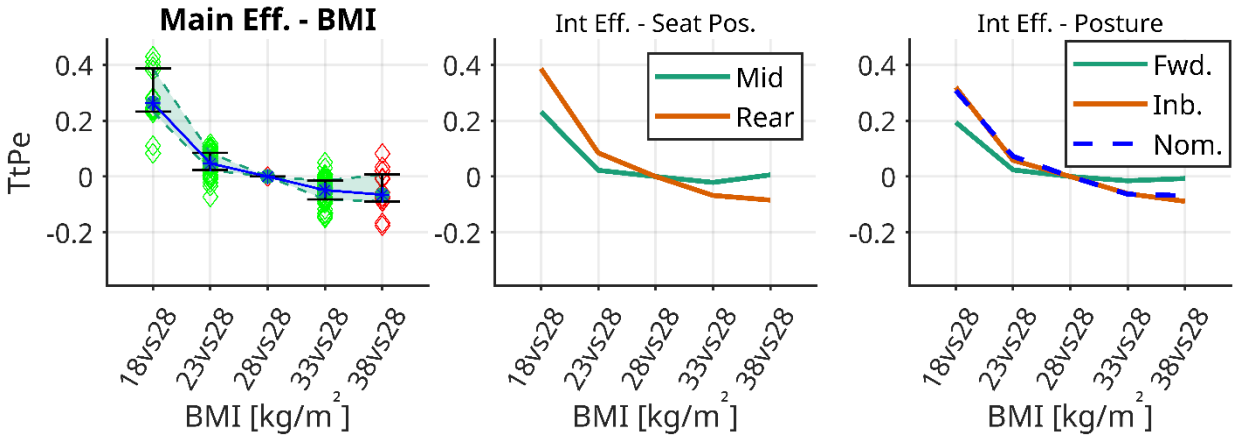

Fig. 6. Influence of BMI on TtPe at 60 ms of the Oncoming Frontal impact simulations. The main effect (on the left) and interaction effects with the seat position (on the centre) and occupant posture (on the right) are presented.

With the ISBP belt configuration, the TtPe had a median value of 0.64 across all setups. The most influential parameters are reported below.

- *BMI*: BMI had a U-Shape effect, with nominal-BMI occupants experiencing the lowest TtPe ratio. Obese occupants had a median increase of 0.08 in TtPe, and underweight occupants experienced a median increase of 0.04 in TtPe, compared to occupants with nominal BMI.
- *Seat Position:* The seat position was influential only as an interaction effect in conjunction with stature. The interaction effect is described under the "*Stature*" bullet point.
- *Posture:* Occupants who were leaning forward experienced a 0.03 reduction in the TtPe ratio.
- *Stature:* When the tall occupants (stature of 190 cm) were in the rearward-positioned seat, their TtPe was reduced by 0.25 on average, as the early contact between the occupant knees and the dashboard limited their pelvis excursion when the seat was in the mid-position.

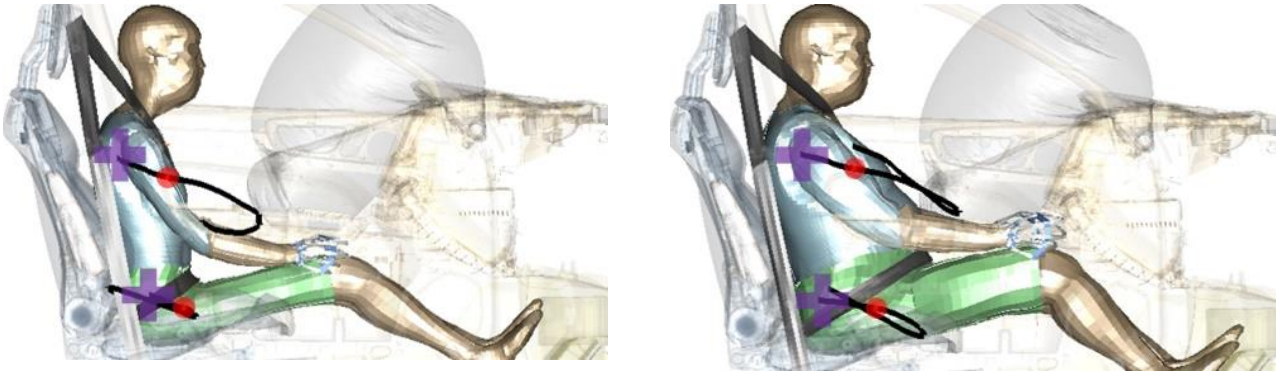

Fig. 7. The position of an underweight (left) and an obese occupant (right), with the traditional belt configuration, at 60 ms of the Oncoming Frontal impact. The torso and pelvis trajectories (black lines) are shown, starting at the purple cross. Red dots are the positions at 60 ms.

Torso Axial Rotation

With the traditional belt configuration, the torso axial rotation, at the 60th ms of the impact, had a median value of 1.6° with IQR of 2°, indicating generally small outboard (towards the RHS of the occupant) rotations.

However, with the ISBP belt, the median rotation was 9.3° (IQR = 8.2°) towards the RHS of the occupant. The occupant's BMI was highly influential for the torso axial rotation. Compared to occupants with a nominal BMI, underweight occupants showed a median increase of 7.5° in outboard axial rotation, while obese occupants had a median reduction of 7.5° in outboard axial rotation with the ISBP belt. As seen in Fig. 8, the torso of the underweight occupant rotated outboard, in contrast to the torso of the obese occupant. Additionally, the posture was influential to the occupant's axial torso rotation, with leaning forward (+4.3°) or inboard (+2.9°) occupants being exposed to larger rotations. Interaction effects between posture and BMI were also found, with underweight occupants having larger rotations when in non-nominal postures (6° when leaning forward and 4.5° when leaning inboard).

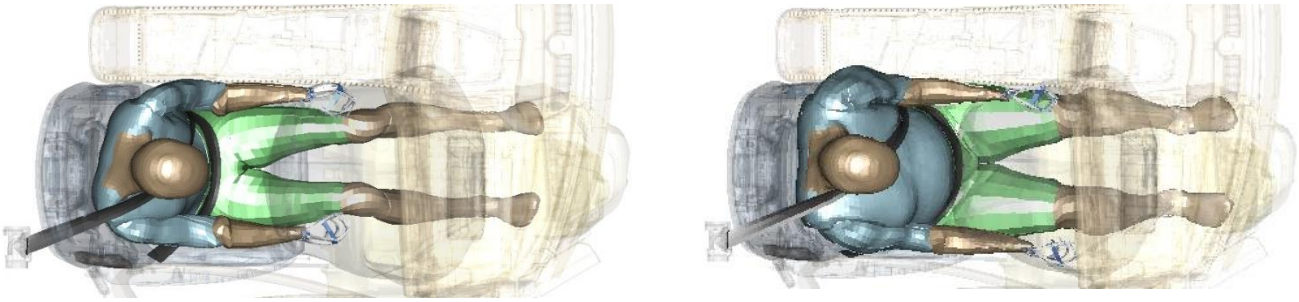

Fig. 8. Illustration of occupant kinematics for an underweight occupant (on the left) and an obese occupant (on the right) at 60 ms of the Oncoming Frontal impact, with the ISBP belt configuration.

Shoulder Belt Interaction

For the simulations in which the lap belt stayed in front of the ASIS (P0 or P1 classification in Table I), further analysis was performed to investigate the shoulder belt interaction in the full-sequence time interval.

Regardless of the belt configuration, the shoulder belt interaction was mainly influenced by the occupant's BMI. The belt placement (SBCP) moved towards the distal end of the clavicle for underweight occupants, while it moved towards the proximal end of the clavicle (neck) for obese occupants. Generally, sliding out of the shoulder belt was observed mainly for tall underweight occupants (Fig. 9). With the occupant in the nominal posture, when the occupant slid out of the belt, it occurred late (in the $t_{R\text{-}10 \rightarrow R+20}$ time interval). Inboard-leaning occupants were more likely to slide out of the shoulder belt (Fig. 9).

Using the traditional belt configuration, the SBCP moved 97% towards the distal end of the clavicle and 26% towards the proximal end of the clavicle for underweight and obese occupants, respectively. Additionally, for each of the 14 cm of stature increase, the SBCP moved 8% more towards the distal end of the clavicle.

With the ISBP belt configuration, the SBCP moved 121% towards the distal end of the clavicle and 33% towards the proximal end of the clavicle for underweight and obese occupants, respectively, compared to occupants with nominal BMI. Additionally, for each of the 14 cm of stature increase, the SBCP moved 14% more towards the

distal end of the clavicle. The shoulder belt interaction classification, for all belt configurations, seat positions and occupant postures can be seen in Appendix E.

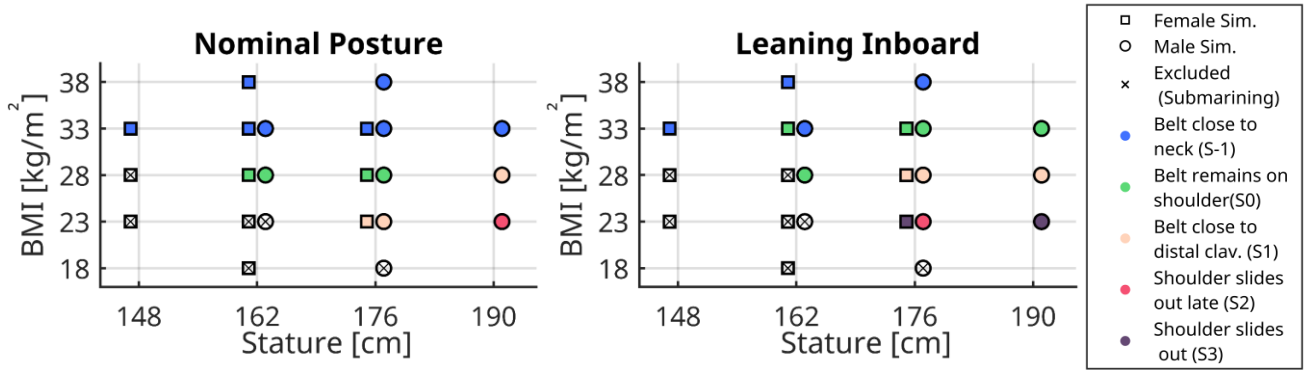

Fig. 9. Shoulder belt to clavicle interaction classification for Oncoming Frontal impact simulations, with the ISBP belt configuration, for occupants in the nominal posture (left) and inboard-leaning posture (right)

Intersection Frontal

No submarining was observed for the Intersection Frontal impacts in any configuration. Additionally, the trends observed in the Oncoming Frontal simulations regarding the TtPe and torso axial rotation mechanisms were consistent with the trends in the Intersection Frontal impacts.

Regarding shoulder belt interaction, similar trends with the Oncoming Frontal impacts were observed, with the SBCP moving towards the distal end of the clavicle more for underweight occupants (median movement 20%) than it did for occupants with nominal BMI. However, no movement towards the proximal end of the clavicle was seen for obese occupants. Leaning forward or inboard increased the SBCP movement towards the distal clavicle end by 10% in the ISBP belt configuration compared to the nominal posture. In the Intersections Frontal impact, the belt remained on the occupant's shoulder for all setups and with both belt configuration.

Far-Side

In the Far-Side impact simulations, the occupant's torso was not exposed to considerable axial rotations with the traditional belt configuration (median 4° inboard, towards the LHS of the occupant).

However, with the ISBP belt, the occupant's torso axial rotation depended on the occupant's BMI. Nominal-BMI occupants experienced negligible rotations (median 1° inboard), while obese occupants rotated inboard (median 5°) and underweight occupants rotated outboard (median 4°). Additionally, the occupant's posture influenced the axial rotations. Leaning forward or inboard reduced the inboard rotations of the torso (approximately by 2°) for obese occupants, while for underweight occupants, the outboard rotations were increased by approximately 2°.

The peak lateral torso excursion was analysed in the full-sequence time interval to examine the influence of the varied parameters on occupant kinematics. With the traditional belt configuration, the median peak lateral torso excursion was 136 mm (IQR=20 mm). Adjusting the seat in the rearward-position reduced the lateral excursions by 15 mm on average. Additionally, inboard-leaning occupants had a median reduction of 13 mm, while forward-leaning occupants were exposed to 5 mm larger excursions compared to occupants in the nominal posture. Compared to nominal-BMI occupants, underweight occupants were associated with smaller torso excursions (-18 mm), while obese occupants were associated with increased torso excursions (+13 mm). Moreover, an 8 mm median increase was seen for females compared to males.

With the ISBP belt, the median peak lateral torso excursion was 135 mm (IQR=27 mm). The lateral excursions were reduced by 14 mm on average in the rearward-position seat. Inboard-leaning occupants experienced reduced (by 19 mm) excursions, while forward-leaning occupants were exposed to 14 mm larger excursions, compared to occupants in the nominal posture. Underweight occupants were associated with reduced torso excursions (-19 mm), while obese occupants were associated with increased torso excursions (+21 mm) compared to nominal-BMI occupants. Additionally, a median increase of 10 mm was seen for females compared to males.

Regardless of belt configuration, no sliding out of the shoulder belt (classified as S3) was observed for occupants in the mid-position seat and nominal posture during the full sequence time interval. Occupants with BMI below nominal and stature at or above nominal were more prone to slide out of the shoulder belt (Fig. 10). The effect was more pronounced for inboard-leaning or forward-leaning occupants (Fig. 10). As seen in Fig. 10, with the

traditional belt configuration and the seat adjusted in the mid-position, 2 out of the 22 occupant sizes slid out of the shoulder belt when they were leaning forward. The shoulder belt interaction classification, for all belt configurations, seat positions and occupant postures can be seen in Appendix F.

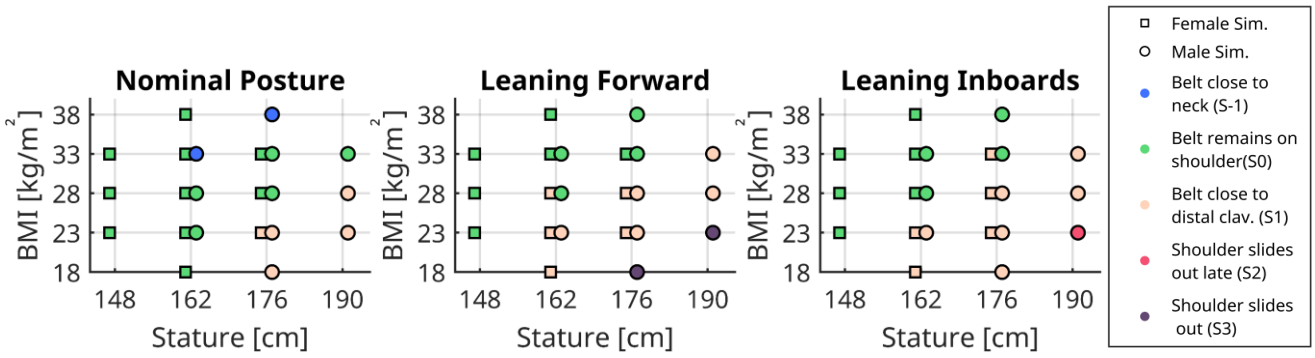

Fig. 10. Classification of shoulder belt to clavicle interaction for occupants in the mid-position and in the nominal (left), leaning forward (centre), and leaning inboard (right) postures during Far-Side impacts with the traditional belt configuration.

With the traditional belt, the most distal belt placement on the occupant's shoulder (SBCP), in the $t_{0\rightarrow R\text{-}10}$ time interval, was increased by 20% when the occupant was leaning forward (Fig. 11) and by 46% when the occupant was leaning inboard. As seen in Fig. 11, the forward-leaning occupant experienced outboard torso rotation, explaining – to some extent – the more distal belt placement. Similarly, a 22% increase in the SBCP was seen for each of the 14 cm of stature increase. Adjusting the seat to the rearward-position increased the SBCP by 24% when the occupant was leaning inboard, compared to the mid-position seat. The SBCP was sensitive to BMI, also depending on the occupant's stature. Taller occupants were generally more sensitive to BMI, with a 58% more distal placement and a 55% more proximal placement for underweight and obese occupant, respectively, compared to nominal-BMI occupants. Shorter underweight occupants experienced a 36% more distal placement compared to nominal-BMI occupants. However, no considerable difference was seen for obese short occupants.

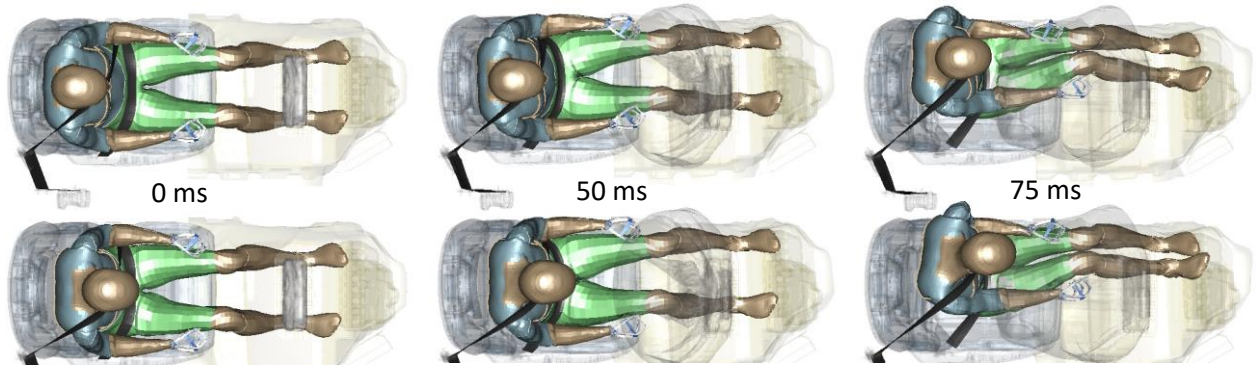

Fig. 11. Illustration of occupant kinematics at the 0, 50, and 75 ms of the Far-Side impact, with the traditional belt configuration, for occupants in the nominal (top) and forward-leaning (bottom) posture.

With the ISBP belt, the SBCP was increased by 24% for forward-leaning occupants and 32% for inboard-leaning occupants, compared to occupants in the nominal posture. Similarly, a 22% increase in SBCP was seen for each of the 14 cm of stature increase. On the contrary, adjusting the seat to the rearward-position reduced the SBCP by 11% compared to the mid-position seat. The SBCP was sensitive to BMI in combination with the occupant's stature. Taller occupants were, in general, more sensitive to BMI, with an 82% more distal placement and a 56% more proximal placement seen for underweight and obese occupant, respectively, compared to nominal-BMI occupants. Shorter underweight occupants experienced a 43% more distal placement compared to nominal-BMI occupants. However, no considerable difference was seen for obese shorter occupants.

IV. Discussion

By exploring the influence of factors, such as occupant variability and restraint configuration, on occupant to belt interaction dynamically during the crash phase, this study extends previous research, which has primarily focused on initial belt fit. A large-scale simulation study was conducted, comprising 792 simulations with 132

setups of varied occupant stature, BMI, sex and posture and seat positions. A sensitivity analysis method was employed to systematically evaluate the influence of the varied parameters across three crash configurations, using a traditional and an Individualised Shoulder Belt Position belt configuration.

Sensitivity analysis, employing one-at-a-time parameter changes at a multitude of input space points, was performed to quantify the influence of the varied parameters on main and interaction effects. The full-factorial DOE was proven useful as interaction effects were generally present, which would not have been made visible otherwise. A novel method quantified and facilitated the analysis of occupant to belt interaction for occupants of diverse anthropometry or subjected to different crash conditions (such as seat position and initial posture). The method, which worked by tracking the motion of the belt relative to anatomical landmarks of the occupant, was also used to auto-classify belt interactions for events such as submarining or sliding out of the shoulder belt. The auto-classified events were also manually inspected and confirmed. Specifically, for the shoulder belt, the belt placement was normalised using the clavicle length, enabling comparisons across individuals of different body shapes and sizes. It should also be mentioned that while the midpoint of the belt was used for the comparisons of the initial shoulder belt fit, the inner edge of the shoulder belt was used for numerical stability reasons during the dynamic analysis of the shoulder belt interaction. This was because identifying the midpoint of the belt when it was almost parallel to the clavicle plane was not stable or meaningful. In future studies, it would be beneficial to investigate further how lap belt interaction can be normalised, enabling comparisons across individuals. In this study, the lap belt interactions were only compared for varied occupant postures and seat positions.

The belt routing was based on the shortest path algorithm over the occupant's body, which was derived from the average of the population (with the selected age, sex, stature, and BMI). Despite that, and despite the attempts to control the belt placement over the clavicle, for the ISBP belt configurations, some variance in the initial belt fit was still present. The observation of a more inboard (towards the buckle) placement of the shoulder belt for obese occupants at the mid-sternum height was consistent with the trends of initial belt fit observed in a laboratory test mock-up [8]. However, even in laboratory studies, occupant characteristics explain a small proportion (40%) of the observed variance in initial belt fit [6]. Real-world variability, such as the occupant's individual body shape, choice of clothes, or preference in the self-selected belt position could further increase the initial belt-fit variance.

Additionally, the ISBP belt configuration was generated by adjusting the D-ring position relative to the occupant's clavicle. The clavicle – as the loaded structure – was selected to study the mechanisms of such a belt configuration. However, from a more practical perspective, the occupant's outer surface (e.g., skin or clothes) would be more suitable.

This study focused on the analysis of occupant to belt interaction, in addition to overall occupant kinematics. Assessment based on injury risk metrics was not included, since the objective targeted seatbelt interaction, whereby the metrics of Lap Belt to ASIS and SBCP were in focus. It is well known that good seatbelt interaction is essential for effective occupant protection. If submarining occurs, the occupant loading changes substantially and detailed injury assessment has a secondary role. Injury assessment may be relevant when no submarining occurs, but mainly in the cases when the occupant remains in the shoulder belt and with the purpose of assessing the overall optimal seatbelt characteristics. However, that was not a part of the objective of the current study.

The included crash pulses exposed the occupants to different combinations of longitudinal and lateral accelerations, and rotations of varied severity, providing insights into the occupant to belt interaction in a wide range of diverse impacts [33]. The sensitivity of both the TtPe ratio and torso axial rotations – the main identified mechanisms – to the parameters examined was consistent across the two frontal crash pulses. Despite the presence of the same mechanisms in both crash pulses, the interaction between the occupant and shoulder belt differed, indicating that the characteristics of the pulse influenced the occupant's interaction with the belt.

In all tested crash configurations, occupants with BMI below nominal and stature above nominal were more likely to slide out of the shoulder belt. Additionally, sliding out of the shoulder belt was more frequently observed in simulations with occupants in the non-nominal posture. However, in the Oncoming Frontal impacts, occupants with BMI and stature below nominal were the ones at higher risk of submarining. Moreover, in the Oncoming Frontal impacts, forward-leaning occupants were less likely to submarine. Those results indicate that different occupant populations might be more or less exposed to slide out of the shoulder belt or to submarine, as well as that they might not be equally influenced by crash conditions, such as the occupant posture.

While the initial belt fit was improved – based on the hypothesis of a mid-shoulder position being optimal – for the ISBP belt compared to the traditional belt configuration, the in-crash occupant responses were not

consistently improved. In the frontal impacts, it was evident that the ISBP belt was highly effective in restraining the occupant's torso. Restraining the torso led, in some cases, to reduced torso forward-pitching motion and increased pelvis excursions which even led to submarining, especially for smaller occupant sizes. The analysis of the traditional belt configuration revealed that the TtPe ratio was highly influenced by the occupant's BMI. More specifically, occupants with BMI below the nominal were subjected to higher TtPe ratios, meaning that their torso was allowed to move forward more than the pelvis, initiating a desirable torso forward-pitching motion in that way. The main mechanism behind this observation is believed to be the altered initial belt fit, which – through different belt angles and initial shoulder to belt gap – essentially acted as a less restrictive belt for the smaller occupants. Nevertheless, even though the initial shoulder belt gap might have added some form of adaptivity to the belt, by making the shoulder belt less restrictive for smaller occupants early in the event; it may not be a robust solution as exemplified by the limited performance (see Fig E.1) in the simulations with non-nominal occupant postures. To achieve robust torso occupant retention, an individualised belt system which allows for early belt to shoulder contact by its placement, but also encompasses belt characteristics with respect to tuned pretensioning and load limiting, would be a desired choice. However, tuning belt characteristics to the individual properties and posture in the specific situation, for the magnitude of combinations, will obviously be a challenging task.

In the Far-Side impacts, the ISBP belt configuration was found to improve torso retention for an HBM with the size of a 50th percentile male, as also noted in [34]. However, this benefit did not extend to occupants with lower BMI or stature. In fact, for smaller occupants, the ISBP belt configuration induced torso axial rotations and resulted in a greater likelihood of sliding out of the shoulder belt. This suggests that the desirable torso retention is not evident for keeping the occupant in the shoulder belt. Additionally, the ISBP belt configuration induced outboard axial rotations on the torso of underweight occupants during the Oncoming Frontal impacts, which were attenuated when the occupants were in non-nominal postures. The observed torso axial rotations could partially be attributed to the initial belt fit relative to the torso's CoG. Generally, occupants with high BMI had the belt positioned more towards the left-hand side of the sternum and a lower torso CoG, which could induce inboard torso axial rotations. The shoulder belt retention was sensitive to BMI, depending on the occupant's stature. However, distinguishing between the effect of stature and sex was difficult, as the overlap of male/female HBMs was limited in the median stature levels, while those effects were mainly seen at the shorter- and taller-ends of the stature scale.

The SAFER HBM v9, which was used in this study, has been validated in previous studies [19–23]. However, the model was not developed to evaluate risk for submarining and lacks validation for this loading. As mentioned in [35], the state-of-the-art HBMs currently face difficulties in accurately representing pelvic rotations, which can play a crucial role in predicting submarining. Additionally, previous studies have shown that this version was somewhat limited in terms of the shoulder belt's interaction biofidelity in far side impacts, which had to be compensated for using a higher friction coefficient [23]. The influence of the varied parameters should thus be seen as trends instead of absolute values. Moreover, the presence of torso axial rotations across all tested crash configurations emphasises the importance of evaluating the biofidelity of axial rotation for HBMs and Anthropometric Test Devices (ATDs) used in the development and evaluation of restraint systems, not only for side impacts [36], but also for frontal impacts.

This study contributes by building knowledge on occupant protection, more specifically, the influence of individualised initial shoulder belt position during impact. Being a large-scale simulation study, it showcased a methodology to handle an analysis including the variations of occupant size and posture and seating position, in addition to the three crash configurations. It included a traditional and an ISBP belt configuration. As demonstrated, changing from a "*one position for all*" to an individualised initial shoulder belt placement as the only restraint variation, may not necessarily lead to an overall improved seatbelt interaction for all, during a crash. In fact, it was shown that depending on the size and posture of the occupant, it might influence the occupant's interaction with the shoulder belt, as well as the lap belt negatively. The variability of the conditions in real-world crashes is immense and is not limited to the factors varied in this study, such as occupant size and posture, seat adjustment, belt routing and crash pulse characteristics. It is evident that individualised occupant protection, requires more than adapting the initial shoulder belt position to account for the specific protection needs of every occupant. In addition to identifying occupant groups of specific concerns and helping to narrow down the scope, the study demonstrates a methodology that can be used in studies investigating other changes in restraint

characteristics. This is essential when moving towards a wider understanding of how to address individualised occupant protection and the challenging task of tuning belt characteristics to the individual properties and posture in the specific situation.

V. CONCLUSIONS

The belt's initial placement over the occupants' shoulder was influential; however, it may not necessarily lead to an overall improved seatbelt interaction as a single parameter. In the frontal impacts, differences in the D-ring position and shoulder belt routing altered the torso to pelvis retention balance and led to different pelvis motion and lap belt interaction. In side impacts, the Individualised Shoulder Belt Position configuration benefited occupants with BMI above nominal, while underweight occupants were more exposed to torso axial rotations, leading to more frequent observation of sliding out of the shoulder belt. Overall, occupants with BMI below nominal and stature above nominal were more likely to slide out of the shoulder belt, while occupants with BMI and stature below nominal were more likely to submarine. Additionally, the occupant's posture influenced the shoulder belt interaction, with inboard or forward-leaning occupants posing a challenge for torso retention.

Individualising the initial shoulder belt placement did not always lead to better occupant kinematics or interaction with the belt, especially for underweight occupants. The presented way of analysing occupant to belt interaction – including multiple setups with diverse occupant sizes, seat positions and occupant postures – identified occupant groups that could potentially be challenging for seatbelt interaction and could facilitate the analysis of additional changes in belt characteristics towards individualised occupant protection.

VI. ACKNOWLEDGEMENT

The work was carried out at SAFER Vehicle and Traffic Safety Centre at Chalmers, Sweden, and partly funded by FFI-Strategic Vehicle Research and Innovation, by Vinnova, the Swedish Energy Agency, the Swedish Transport Administration and the Swedish vehicle industry. The authors are grateful to Karl-Johan Larsson (Chalmers University of Technology and Autoliv Research, Sweden) for his valuable support in the HBM morphing process and for all the constructive discussions.

VII. REFERENCES

[1] Adomeit D, Heger A. (1975) Motion sequence criteria and design proposals for restraint devices in order to avoid unfavorable biomechanic conditions and submarining. Stapp Car Crash Journal, **19**: pp.139-165. doi.org/10.4271/751146.

[2] Fong C K, Keay L, Coxon K, Clarke E, Brown J. (2016) Seat belt use and fit among drivers aged 75 years and older in their own vehicles. Traffic Injury Prevention, **17**(2): pp.142-50. doi.org/10.1080/15389588.2015.1052420.

[3] Osvalder A L, Bohman K, Lindman M, Ankartoft S. (2019) Seat belt fit and comfort for older adult front seat passengers in cars. Proceedings of the IRCOBI Conference, Florence, Italy: pp.32–43. IRC-19-12

[4] Bohman K, Osvalder A L, Ankartoft R, Alfredsson S. (2019) A comparison of seat belt fit and comfort experience between older adults and younger front seat passengers in cars. Traffic Injury Prevention, **20**(sup2): pp.S7-S12, DOI: 10.1080/15389588.2019.1639159.

[5] Reed M, Ebert S, Hallman J. (2013) Effects of Driver Characteristics on Seat Belt fit. Stapp Car Crash Journal, **57**: pp.43-57. doi.org/10.4271/2013-22-0002.

[6] Jones M L H, Ebert S M, *et al.* (2021) Effect of Class I–III obesity on driver seat belt fit. Traffic Injury Prevention, **22**(7): pp.547–552. doi:10.1080/15389588.2021.1945590.

[7] Reed M P, Ebert S M, Jones M L H. (2019) Posture and belt fit in reclined passenger seats. Traffic Injury Prevention, **20**(sup1): pp.S38-S42. doi: 10.1080/15389588.2019.1630733.

[8] Jones M L H, Ebert S M, Hu J, Reed M P. (2017) Effects of high levels of obesity on lap and shoulder belt paths. Proceedings of the IRCOBI Conference, Antwerp, Belgium: pp.317–326. IRC-17-50.

[9] Ejima S, Holcombe S A, *et al.* (2016) Application of Analytic Morphomics for Belted Elderly Occupants in Frontal Crashes. Proceedings of IRCOBI Conference, Malaga, Spain: pp.858–869. IRC-16-105.

[10] Hu J, Zhang K, Reed M P, Wang J T, Neal M, Lin C H. (2019) Frontal crash simulations using parametric human models representing a diverse population. Traffic Injury Prevention, **20**(sup1): pp.S97–S105. doi:10.1080/15389588.2019.1581926.

[11]Perez-Rapela D, Forman J L, Huddleston S H, Crandall J R. (2020) Methodology for vehicle safety development and assessment accounting for occupant response variability to human and non-human factors. Computer Methods in Biomechanics and Biomedical Engineering, **24**(4): pp.384–399. doi:10.1080/10255842.2020.1830380.

[12]Wang Y, Bai Z, *et al.* (2015) A simulation study on the efficacy of advanced belt restraints to mitigate the effects of obesity for rear-seat occupant protection in frontal crashes. Traffic injury prevention, **16**(sup1): pp.S75-S83. doi.org/10.1080/15389588.2015.1010722.

[13]Joodaki H, Gepner B, Kerrigan J. (2021) Leveraging machine learning for predicting human body model response in restraint design simulations. Computer Methods in Biomechanics and Biomedical Engineering, **24**(6): pp.597–611. doi:10.1080/10255842.2020.1841754.

[14]Boyle K, Fanta A, *et al.* (2020) Restraint systems considering occupant diversity and pre-crash posture. Traffic Injury Prevention, **21**(sup1): pp.S31–S36. doi:10.1080/15389588.2021.1895989.

[15]Joodaki H, Gepner B, Lee S H, Katagiri M, Kim T, Kerrigan J. (2021) Is optimized restraint system for an occupant with obesity different than that for a normal BMI occupant? Traffic Injury Prevention, **22**(8): pp.623–628. doi:10.1080/15389588.2021.1965131.

[16]Miller M, Perez-Rapela D, Gepner D, Edwards M, Jermakian J, Forman J. (2021) A methodology for large-scale parametric evaluation of child booster seats. Proceedings of the IRCOBI Conference, online: pp.593–615. IRC-21-62.

[17]Baker G H, Mansfield J A, Bolte J H. (2022) Influence of initial belt torso contact on the kinematics and kinetics of booster-seated ATDs in frontal impacts. Proceedings of the IRCOBI Conference, Porto, Portugal: pp.479–518. IRC-22-70.

[18]Östh J, Bohman K, Jakobsson L. (2020) Evaluation of Kinematics and Restraint Interaction when Repositioning a Driver from a Reclined to an Upright Position Prior to Frontal Impact using Active Human Body Model Simulations. Proceedings of the IRCOBI Conference: pp.358–380. IRC-20-50.

[19]Pipkorn B, Iraeus J, Björklund M, Bunketorp O, Jakobsson L. (2019) Multi-scale validation of a rib fracture prediction method for human body models. Proceedings of the IRCOBI Conference, Florence, Italy: pp.175–192. IRC-19-34.

[20]Iraeus J, Pipkorn B. (2019) Development and validation of a generic finite element ribcage to be used for strain-based fracture prediction. Proceedings of the IRCOBI Conference, Florence, Italy:193–210. IRC-19-35.

[21]Larsson K J, Pipkorn B, *et al.* (2019) Evaluation of the benefits of parametric human body model morphing for prediction of injury to elderly occupants in side impact. Proceedings of the IRCOBI Conference, Florence, Italy: pp.150–174. IRC-19-33.

[22]Mroz K, Östling M, *et al.* (2020) Effect of Seat and Seat Belt characteristics on the Lumbar Spine and Pelvis Loading of the SAFER Human Body Model in reclined Postures. Proceedings of the IRCOBI Conference: pp.470–486. IRC-20-58.

[23]Pipkorn B, Larsson K J, *et al.* (2018) Occupant protection in far-side impacts. Proceedings of the IRCOBI Conference, Athens, Greece: pp.76–105. IRC-18-16.

[24]Leledakis A, Östh J, Iraeus J, Davidsson J, Jakobsson L. (2022) The influence of occupant's size, shape and seat adjustment in frontal and side impacts. Proceedings of the IRCOBI Conference, Porto, Portugal:549–584. IRC-22-75.

[25]Hwang E, Hallman J, Klein K, Rupp J, Reed M, Hu J. (2016) Rapid Development of Diverse Human Body Models for Crash Simulations through Mesh Morphing. SAE Technical Paper 2016-01-1491. doi:10.4271/2016-01-1491.

[26]Larsson K J, Pipkorn B, Iraeus J, Forman J, Hu J. (2021) Evaluation of a diverse population of morphed human body models for prediction of vehicle occupant crash kinematics. Computer Methods in Biomechanics and Biomedical Engineering, **25**(10): pp.1125-1155. doi:10.1080/10255842.2021.2003790.

[27]Leledakis A, Östh J, Davidsson J, Jakobsson L. (2021) The influence of car passengers' sitting postures in intersection crashes. Accident Analysis & Prevention, **157**. doi:10.1016/j.aap.2021.106170.

[28]Östh J, Pipkorn B, Forsberg J, Iraeus J. (2021) Numerical Reproducibility of Human Body Model Crash Simulations. Proceedings of the IRCOBI Conference, online: pp.431–441. IRC-21-51.

[29]Reed, M. P., Ebert, S. M., Jones, M. L. H., Hallman, J. J. (2020) Prevalence of non-nominal seat positions and postures among front-seat passengers. Traffic Injury Prevention, 21(sup1): pp.S7–S12. doi:10.1080/15389588.2020.1793971.

[30]Bohman K, Jakobsson L, Nurbo P, Olander A, Andersson A. (2020) Lateral movement of front seat passengers in everyday traffic. Proceedings of the IRCOBI Conference: pp.410–426. IRC-20-53.

[31]Poulard D, Subit D, Donlon J-P, Kent R W. (2015) Development of a computational framework to adjust the pre-impact spine posture of a whole-body model based on cadaver tests data. Journal of Biomechanics, **48**(4): pp.636–643. doi:10.1016/j.jbiomech.2014.12.050.

[32]Iraeus J, Lindquist M. (2016) Development and validation of a generic finite element vehicle buck model for the analysis of driver rib fractures in real life nearside oblique frontal crashes. Accident Analysis & Prevention, 95(A): pp.42-56. doi.org/10.1016/j.aap.2016.06.020.

[33]Leledakis A, Lindman M, Östh J, Wågström L, Davidsson J, Jakobsson L. (2021) A method for predicting crash configurations using counterfactual simulations and real-world data. Accident Analysis & Prevention, **150**. doi:10.1016/j.aap.2020.105932.

[34]Umale S, Yoganandan N, Pintar F A, Arun M W J. (2018) Factors influencing the effectiveness of occupant retention under far-side impacts: A parametric study. Journal of the Mechanical Behavior of Biomedical Materials, **84**: pp.235–248. doi:10.1016/j.jmbbm.2018.05.021.

[35]Gepner B D, Perez-Rapela D, Forman J L, Ostling M, Pipkorn B, Kerrigan J R. (2022) Evaluation of GHBMC, THUMS and SAFER Human Body Models in Frontal Impacts in Reclined Postures. Proceedings of the IRCOBI Conference, Porto, Portugal:116–143. IRC-22-27.

[36]Forman J L, Lopez-valdes F, *et al.* (2013) Occupant Kinematics and Shoulder Belt Retention in Far-Side Lateral and Oblique Collisions: A Parametric Study. Stapp Car Crash Journal, **57**: pp.343-385. doi:10.4271/2013-22-0014

Appendix A

Belt Fit for Varying D-ring Positions

For the ISBP belt configuration, the D-ring position was adjusted in relation to the midpoint of the HBM's clavicle (Fig A.1). The D-ring was kept at a constant distance from the clavicle of 300 mm and at an angle of 35° relative to the sagittal plane and 10° relative to the transverse plane (Fig. A.2-3). The angles were chosen with the goal of placing the shoulder belt in a "*theoretically good*" initial position over the occupant's mid-shoulder, regardless of the occupant's size (Fig A.4). The selected angle (35°) generated a mid-shoulder belt placement for most occupants. However, especially for short, obese occupants, the belt placement was closer to the neck.

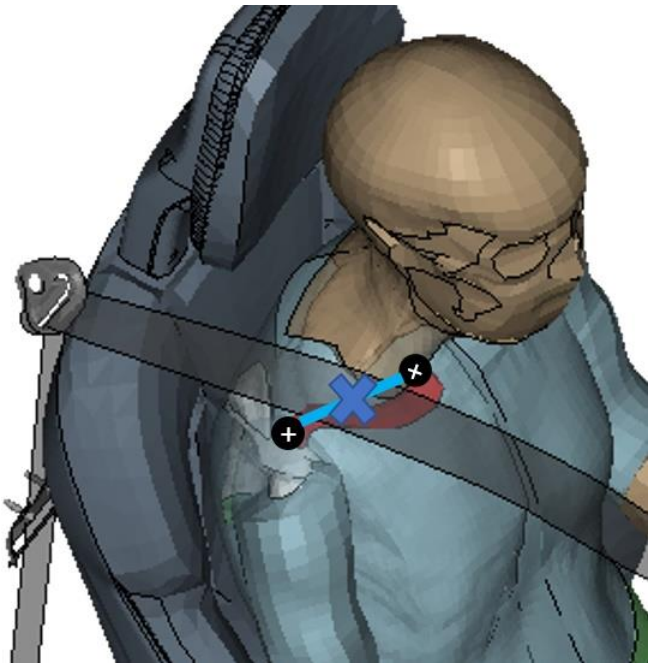

Fig. A.1. The clavicle proximal and distal ends are highlighted with black spheres, and the mid-point can be seen with the blue "*X*".

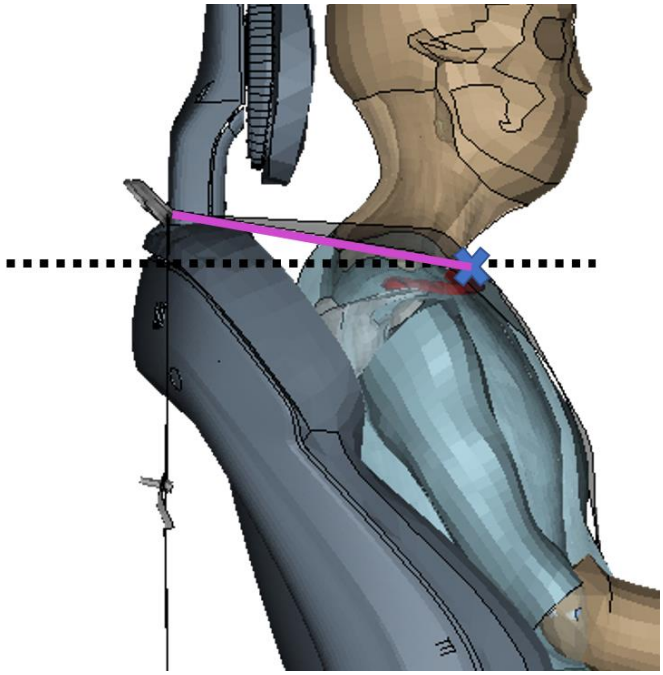

Fig. A.2. Belt angle relative to the transverse plane (dashed line).

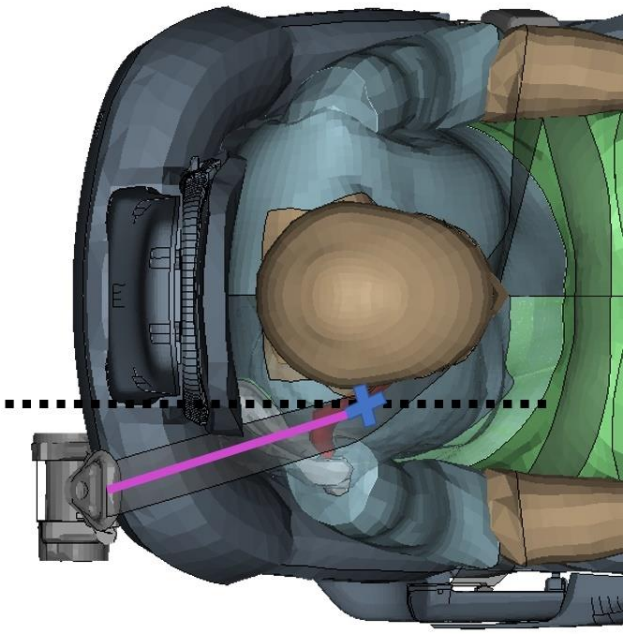

Fig. A.3. Belt angle relative to the sagittal plane (dashed line).

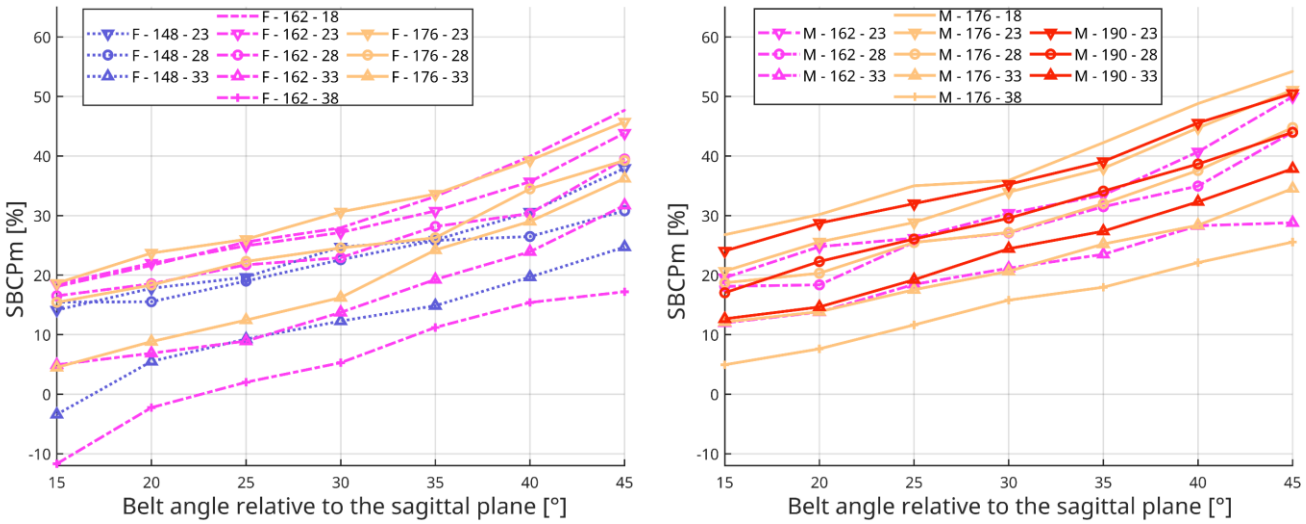

Fig. A.4. The shoulder Belt Clavicle Placement midpoint (SBCPm) for the included 11 Female (on the left) and 11 Male (on the right) HBMs, for the investigated belt angles relative to the sagittal plane. Higher belt angle correlated with higher SBCPm, which indicated a more distal shoulder belt placement on the clavicle. The occupant's size influenced the SBCPm. Shorter and obese occupants had a more proximal belt placement, while taller and underweight occupants had a more distal belt placement.

Appendix B

Belt Fit Calculation

The seatbelt interaction was quantified, in terms of the belt's position on the occupant, by measuring the distance of the belt relative to the occupants' anatomical landmarks. Euclidean planes were constructed using three anatomical landmarks of the pelvis, thoracic cage and clavicle. The motion of the belt in those planes was measured relative to the anatomical landmark of interest prior to the impact, for the initial belt fit, and over time, for the belt interaction. For the lap belt, the left and right ASIS were used. For the shoulder belt, the HBM's sternum and the distal end of the right clavicle were used.

The pelvis plane was defined using a) the most superior-anterior point of the pubic symphysis, b) the most superior point of the median sacral crest, and c) the most inferior-anterior point of the pubic symphysis (Fig B.1). The plane was then offset, so that the origin would coincide with the left or right ASIS, for the lap belt interaction analysis over the left and right ASIS, respectively. The orientation of the plane followed the three landmarks defining it, over time.

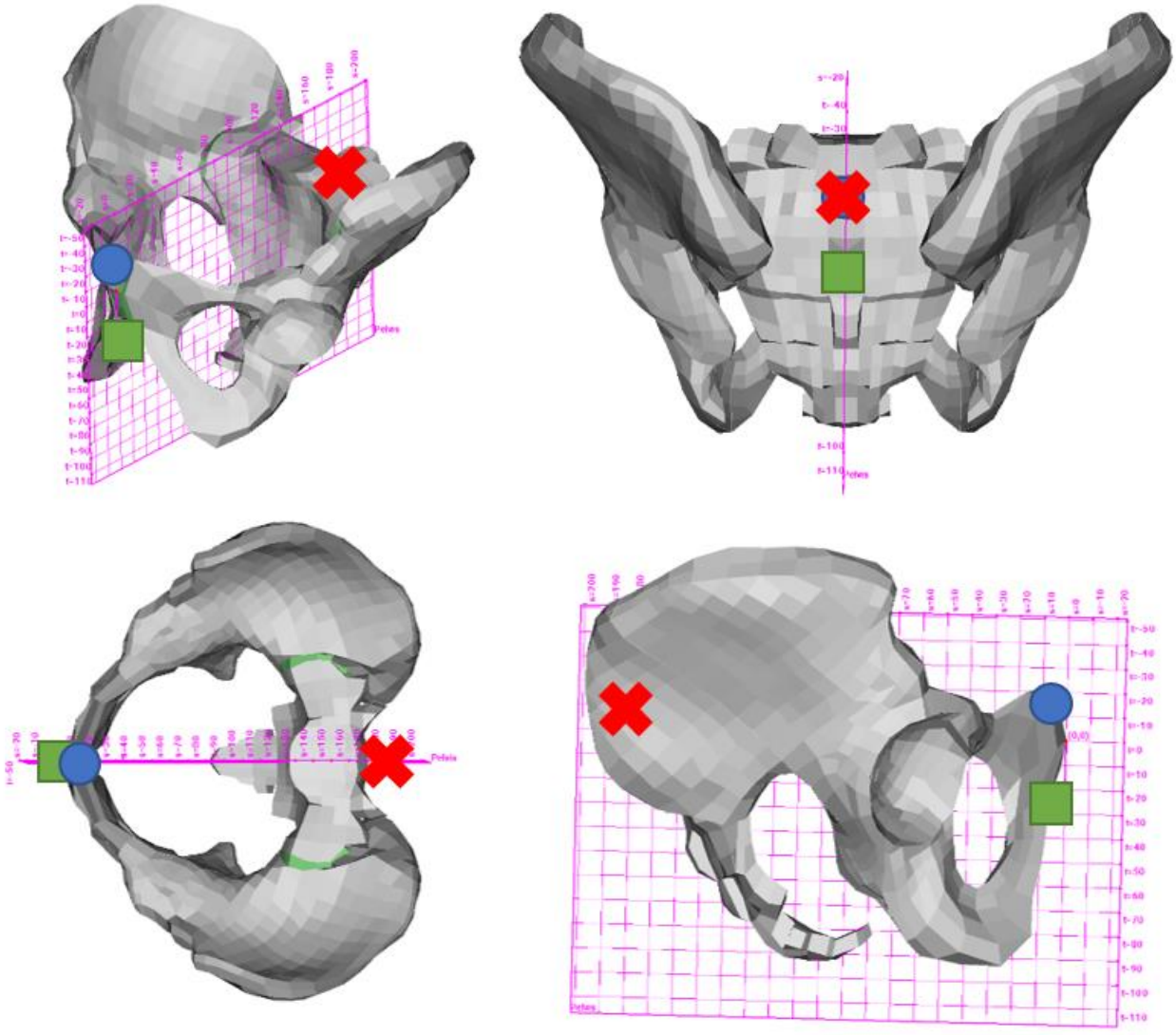

Fig. B.1. Four views of the pelvis and the plane defined on it. The most superior-anterior point of the pubic symphysis can be seen with the blue dot. The most superior point of the median sacral crest is illustrated with the red X. The most inferior-anterior point of the pubic symphysis is visualised with a green square.

The clavicle plane was defined using a) the most distal-anterior point of the clavicle, b) the most proximal-anterior point of the clavicle, and c) the most posterior-anterior point of the clavicle (Fig B.2).

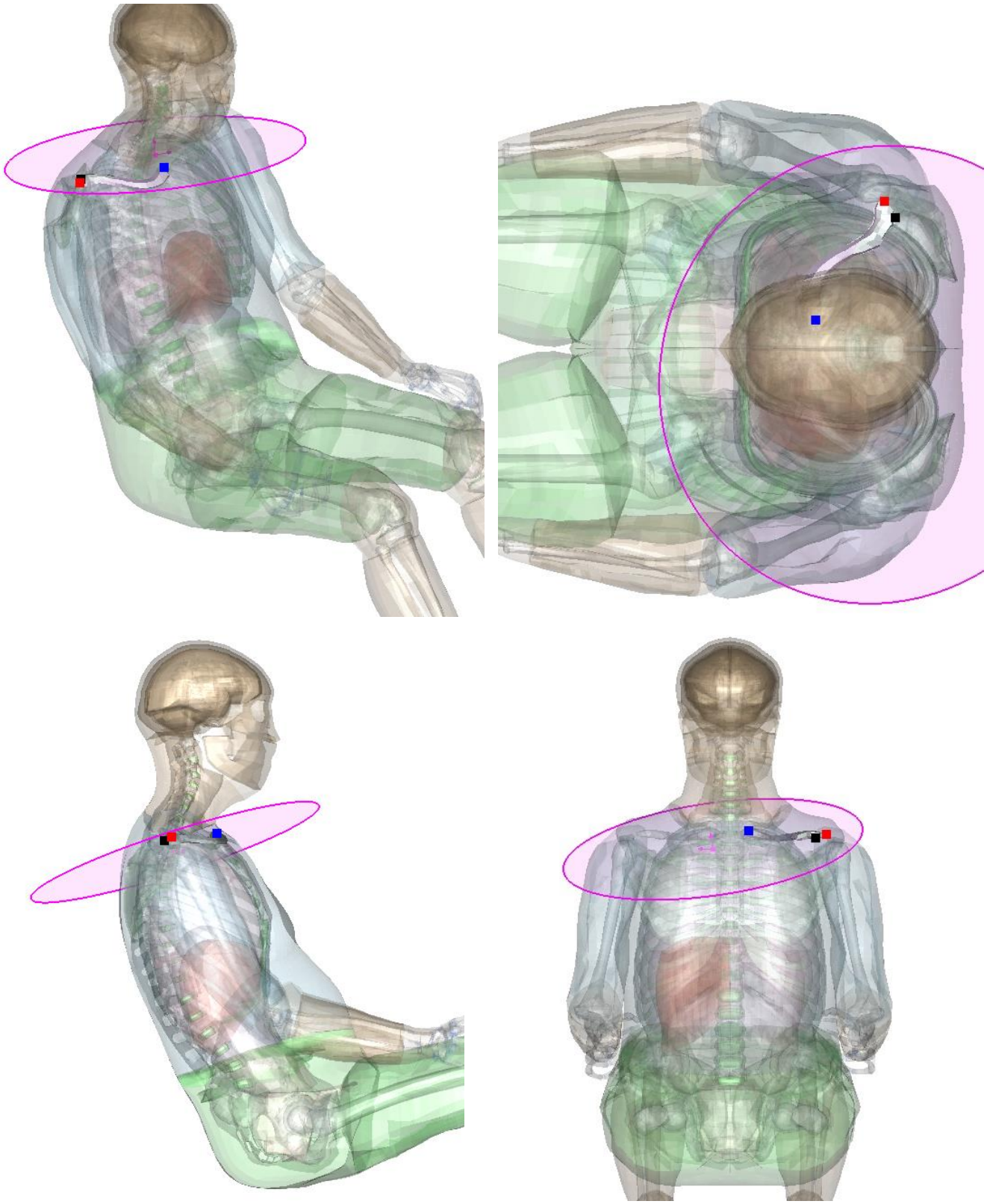

Fig. B.2. Four views of the occupant with the clavicle and the plane defined on it. The most distal-anterior point of the clavicle can be seen with the red square. The most distal-posterior point of the clavicle is illustrated with the black square. The most posterior-anterior point of the clavicle is visualised with a blue square.

The sternum plane was defined using a) the middle of gladiolus, at the fourth rib height, b) the posterior-superior point of the T6 vertebral foramen, and c) the most distal point of the T6 left transverse process (Fig B.3).

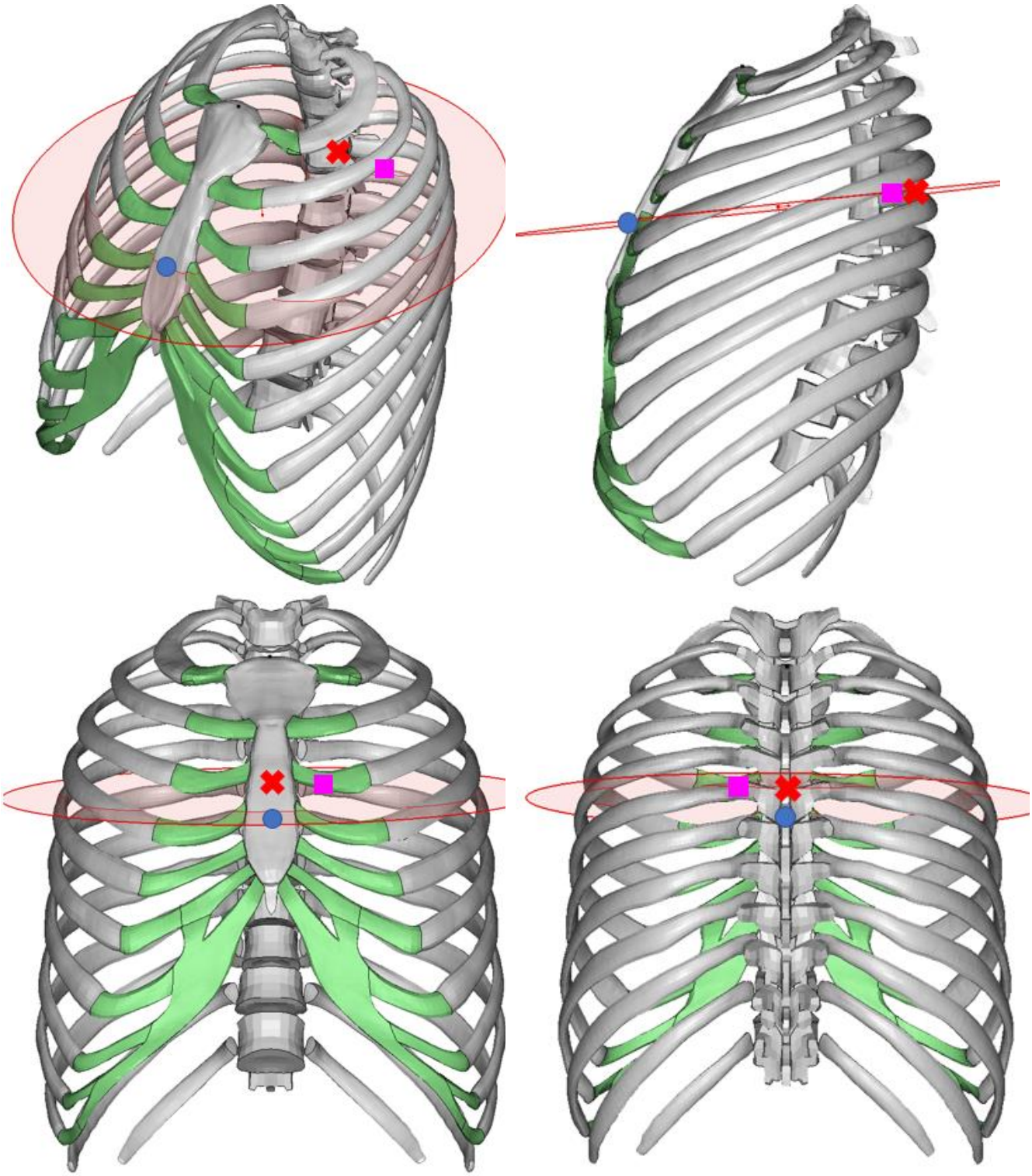

Fig. B.3. Four views of the thoracic cage and the sternum plane defined on it. The middle of gladiolus, at the fourth rib height, can be seen with the blue circle. The posterior-superior point of the T6 vertebral foramen is illustrated with the red X. The most distal point of the T6 left transverse process is visualised with the magenta square.

An example of the lap and shoulder belt interaction analysis during an Oncoming Frontal impact can be seen in Fig B.4.

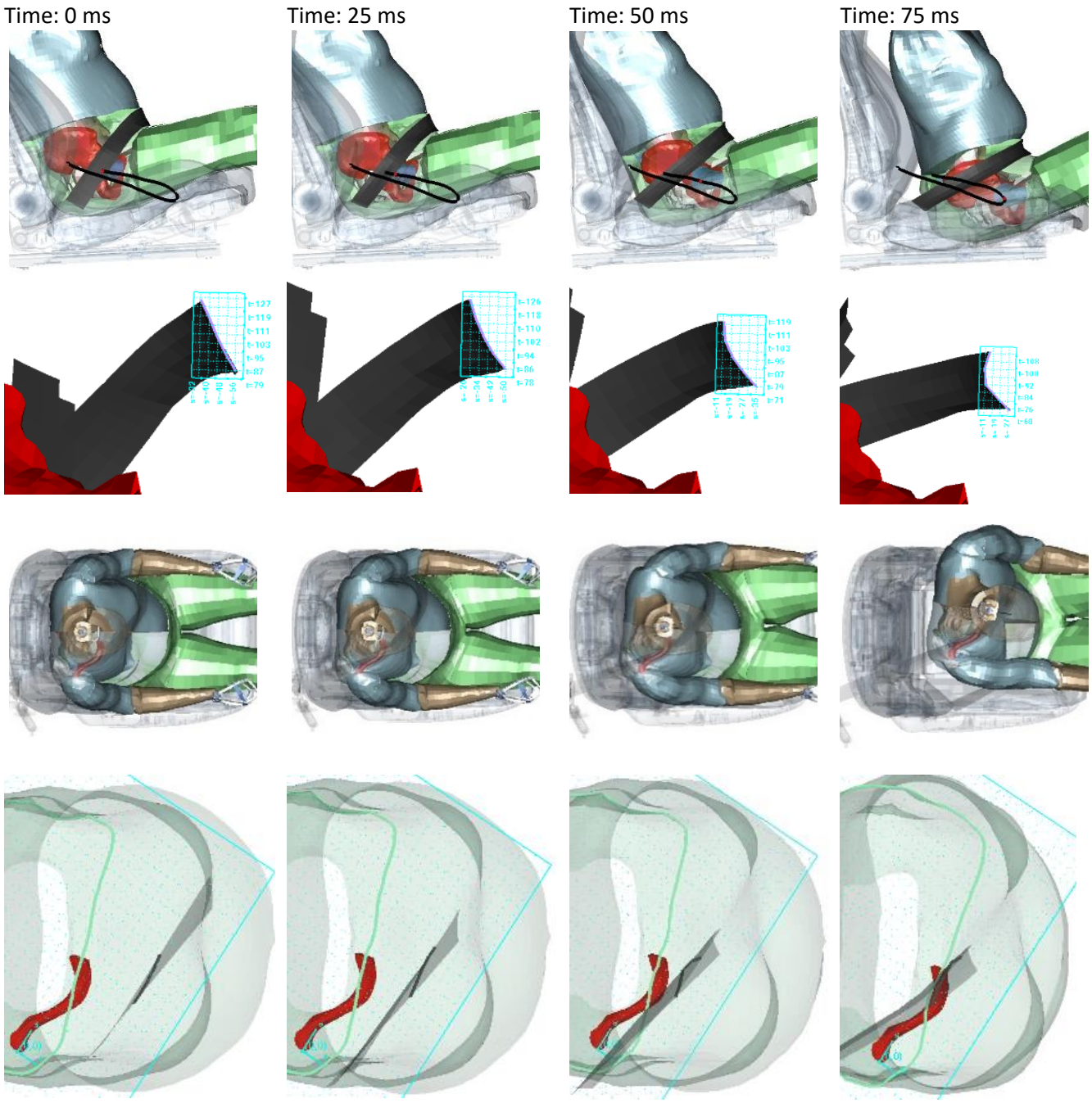

Fig. B.4. Example of the lap belt and shoulder placement analysis over time, at 0ms, 25 ms, 50 ms, and 75 ms of the Oncoming Frontal simulation.

Appendix C

Initial Belt Fit for the Occupant Sizes

For occupants with high BMI, the shoulder belt shifted laterally towards the Left-Hand Side (LHS) at the mid-sternum, moving it on average by 52 mm and 70 mm for obese occupants compared to occupants with nominal BMI for the traditional and ISBP belt configuration, respectively. Contrary to this, no considerable difference was observed for underweight occupants, with either of the belt configurations. Additionally, the occupant's BMI was influential for the belt placement over the clavicle. The belt was shifted towards the neck of the occupants as BMI increased, with a median change of -22% SBCPm for obese occupants compared to occupants with nominal BMI, regardless of belt configuration. The opposite trend was observed for underweight occupants, with the belt moving towards the distal end of the clavicle by 3% and 9% on average, for the Traditional and ISBP belt configuration, respectively.

Increasing the occupant's stature, contrary to BMI, positioned the shoulder belt towards the RHS of the sternum, on average, by 13 mm, regardless of the belt configuration. Furthermore, for the traditional belt configuration, the belt placement over the clavicle was shifted towards the distal end of the clavicle for taller occupants, with an average increase of 15% SBCPm for each of the 14 cm of stature increase.

While no clear trends were observed between the occupant's sex and belt placement with the ISBP belt configuration; however, the belt placement was influenced in the traditional belt configuration. More specifically, the belt was placed towards the RHS of the sternum (on average by 11 mm when compared to males of the same stature and BMI). Moreover, the belt was, on average, 10% closer to the neck for female occupants than for male occupants with the traditional belt configuration.

No influence was seen for the seat's fore-aft position on the initial belt fit when using the ISBP belt configuration. However, with the traditional belt configuration, the seat's position was found to affect the longitudinal placement (gap) of the shoulder belt on the clavicle. A gap was observed between the occupant and the shoulder belt, in some cases, which was increased in the rearward-positioned seat, particularly for occupants with high BMI and low stature. As an example, the largest gap was observed for a female with a stature of 148 cm and BMI 33, positioned at the rearward-position seat, and was equal to 84 mm.

The occupant's posture influenced the belt fit for both belt configurations. Generally, the belt was positioned more towards the RHS of the sternum and away from the neck for inboard-leaning occupants. For forward-leaning occupants, the belt was positioned more towards the LHS of the sternum and away from the neck. The belt fit was more influenced by the occupant's posture using the traditional belt configuration compared to the ISBP one. With the traditional belt configuration, the belt was positioned on average 20 mm towards the RHS of the sternum and 35% more towards the distal end of the clavicle when leaning inboard. As well, the gap observed between the occupant and the belt at the clavicle height, was reduced by an average of 24 mm when the occupant was leaning forward.

The placement of the shoulder belt's midpoint on the occupant's clavicle (SBCPm) was used to classify the initial shoulder belt fit, as seen in Table C.I. The classification for the traditional and ISBP belt configurations can be seen in Fig C.1 and C.2, respectively.

TABLE C.I
SHOULDER BELT FIT CLASSIFICATION

Classification	*Interpretation*
Belt on the neck	The midpoint of the shoulder belt was located before 0% SBCPm (proximal end of the clavicle)
Belt close to the neck	The midpoint of the shoulder belt is located between 0% and 25% SBCPm
Mid-Shoulder placement	The midpoint of the shoulder belt is located between 25% and 50% SBCPm
Belt on the 3rd quarter of the clavicle	The midpoint of the shoulder belt is located between 50% and 75% SBCPm
Belt close to shoulder	The inner edge of the shoulder belt moves past the 75% SBCPm (close to the distal end of the clavicle)

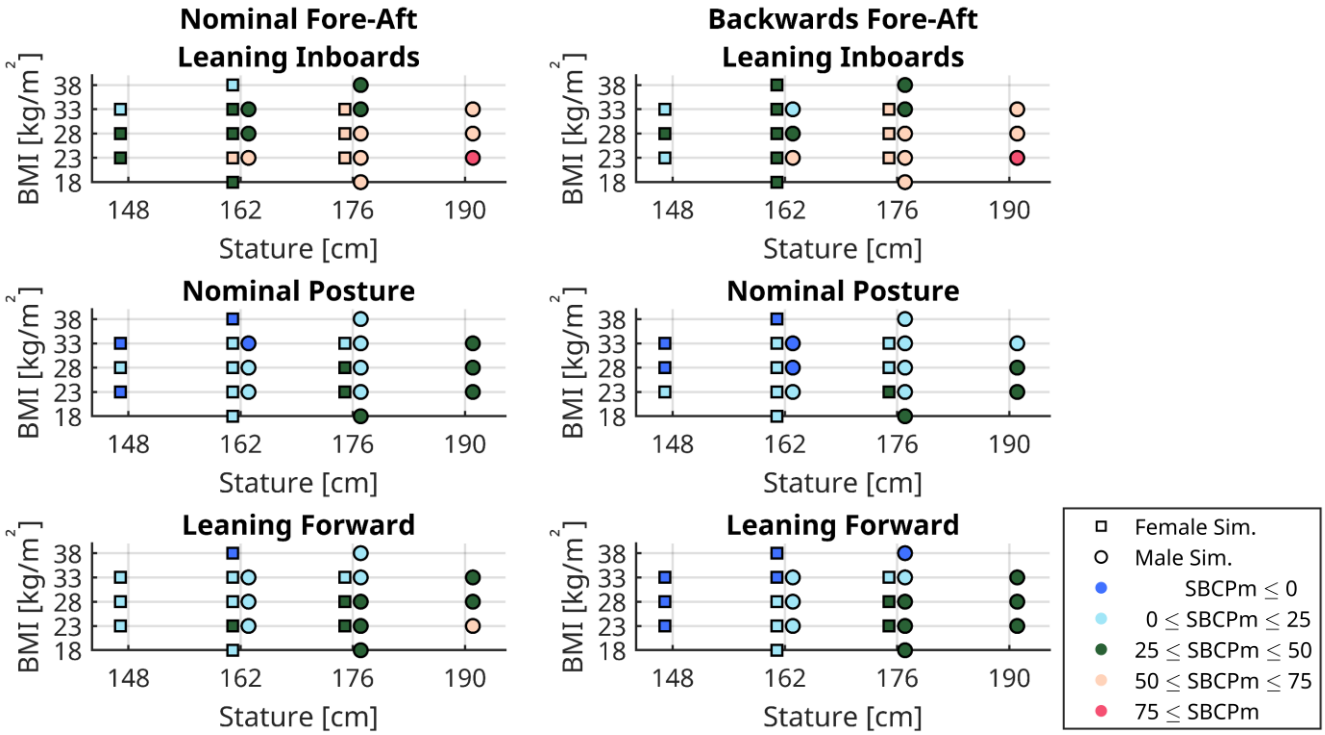

Fig. C.1. Shoulder belt fit classification with the traditional belt configuration.

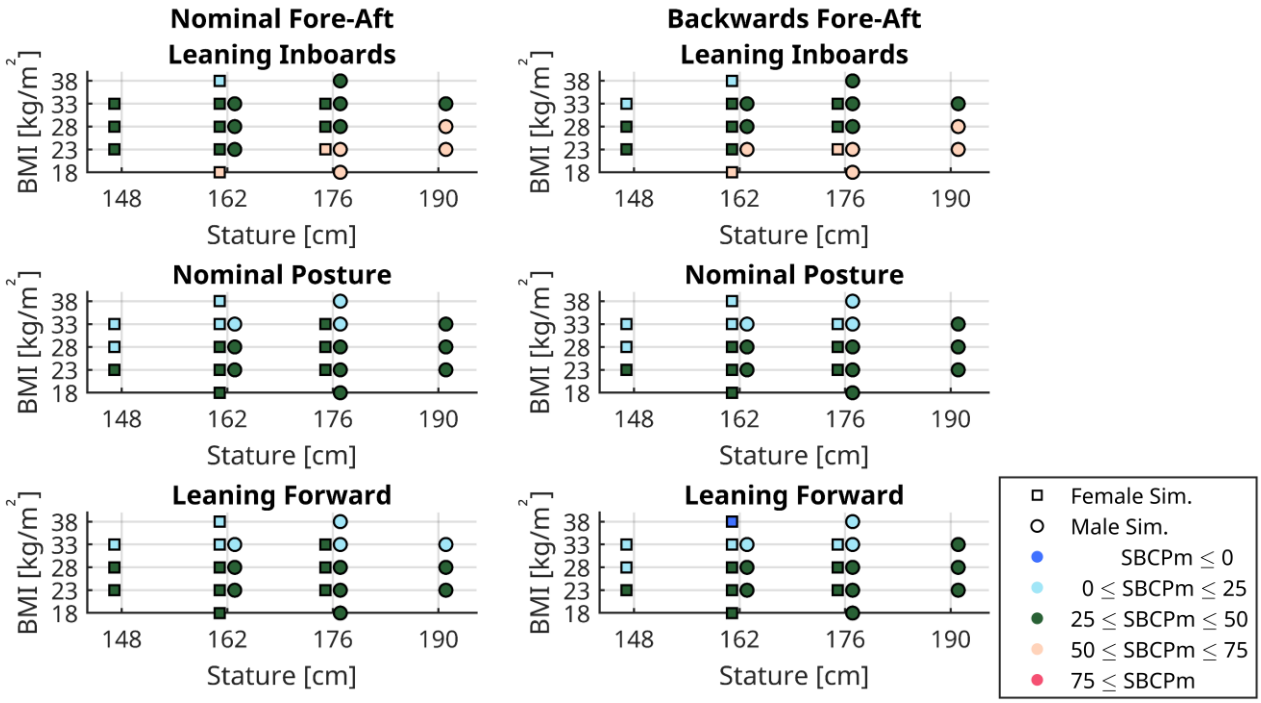

Fig. C.2. Shoulder belt fit classification with the ISBP belt configuration.

Appendix D

Lap Belt to ASIS Interaction Classification, Oncoming Frontal Impacts

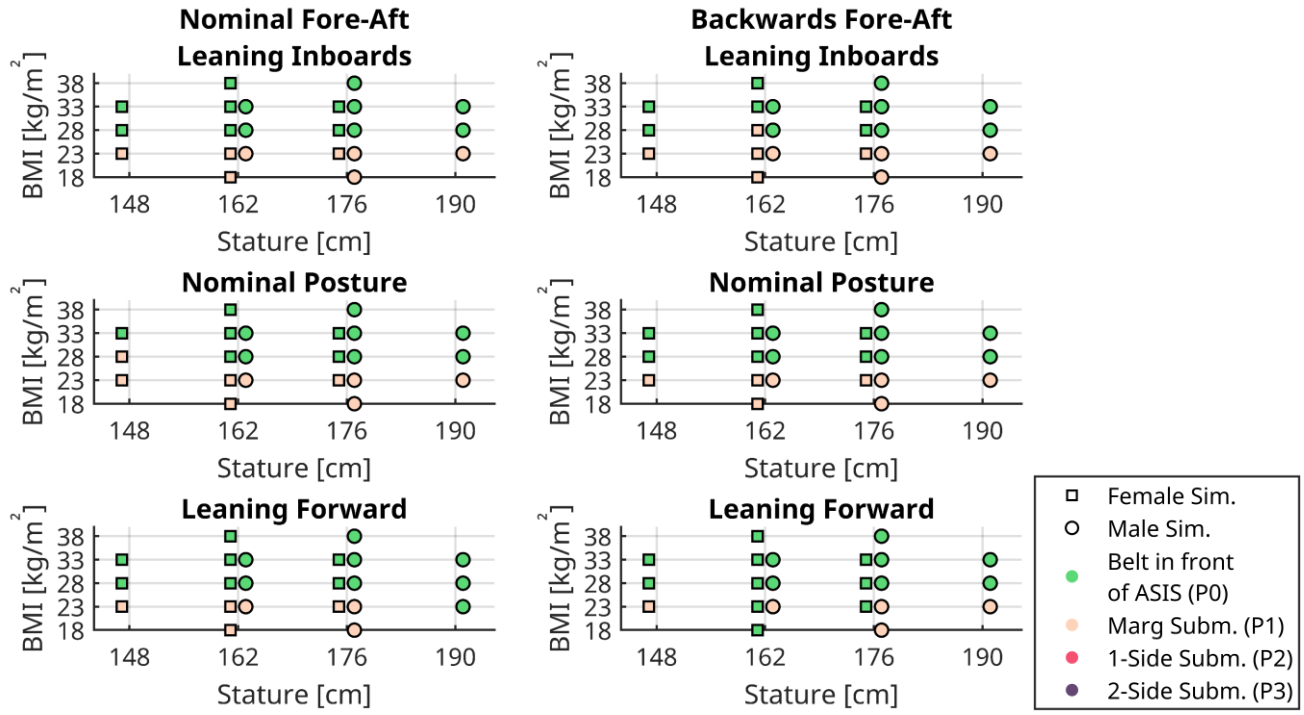

Fig. D.1. Lap Belt to ASIS interaction classification with the traditional belt configuration.

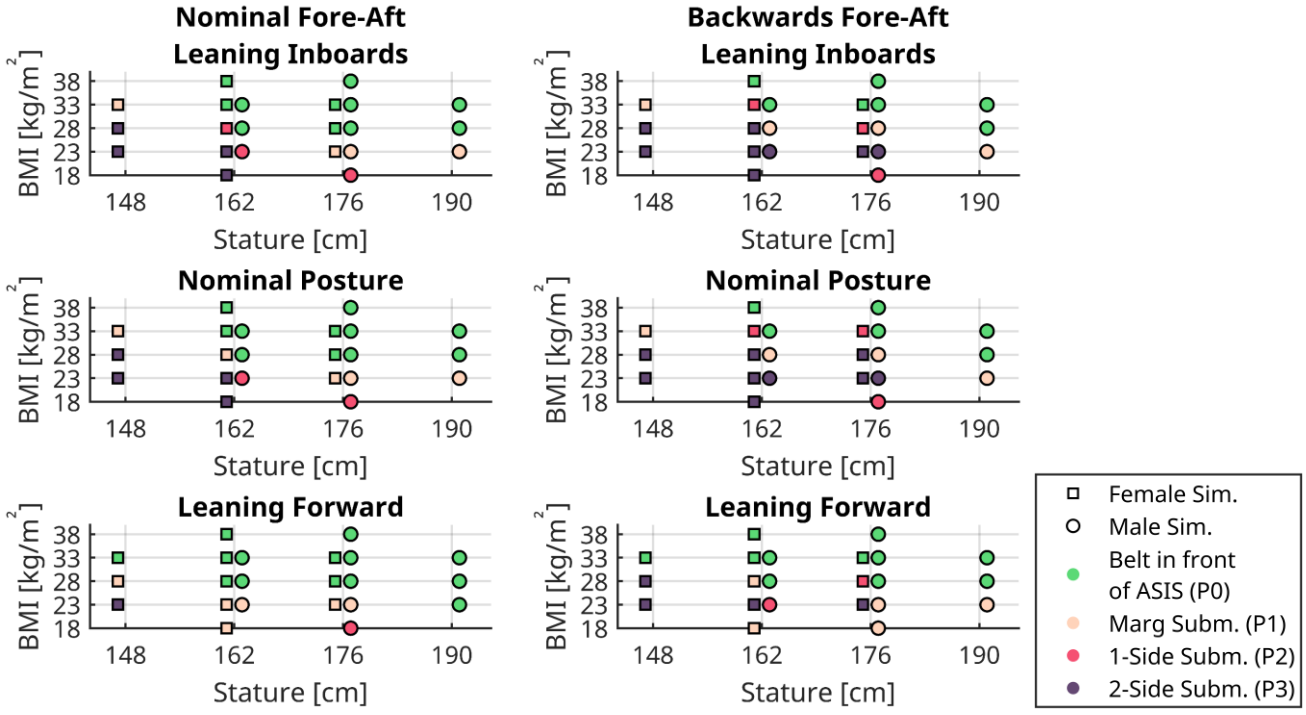

Fig. D.2. Lap Belt to ASIS interaction classification with the ISBP belt configuration.

Appendix E

Shoulder Belt to Clavicle Interaction Classification, Oncoming Frontal Impacts

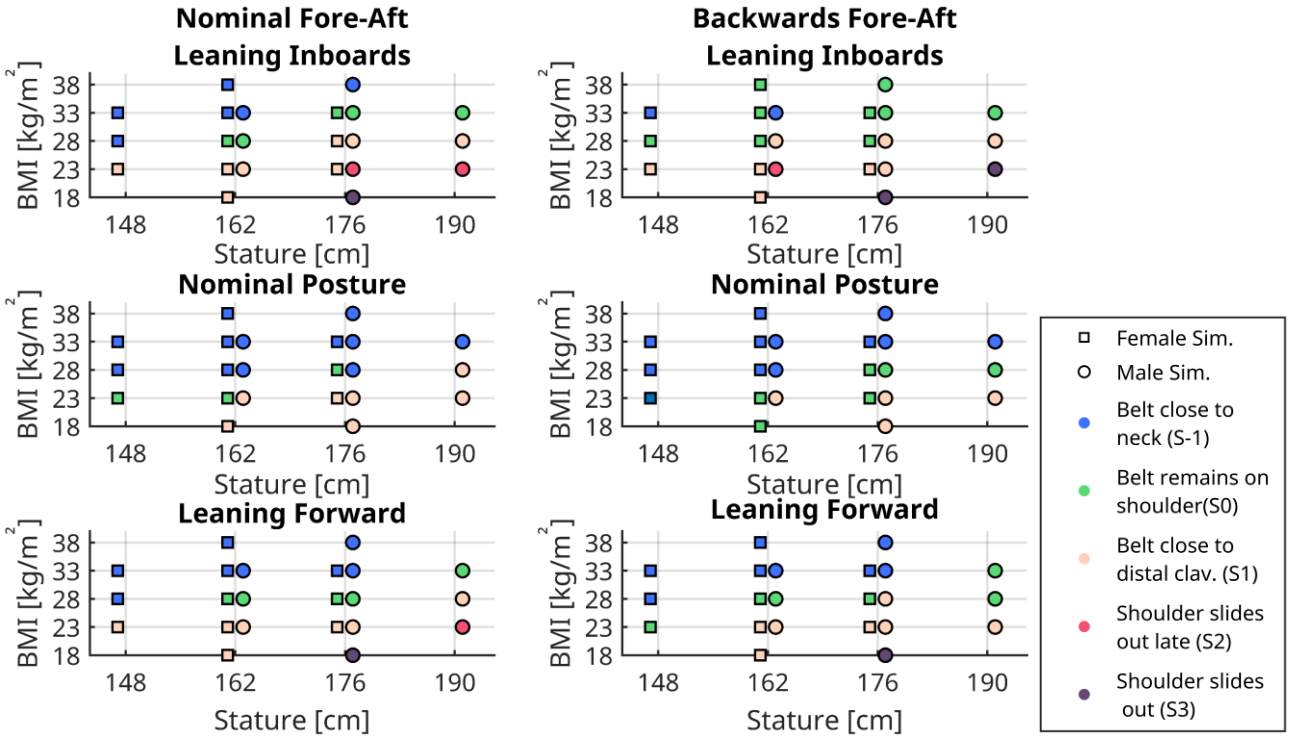

Fig. E.1. Shoulder belt to clavicle interaction classification with the traditional belt configuration.

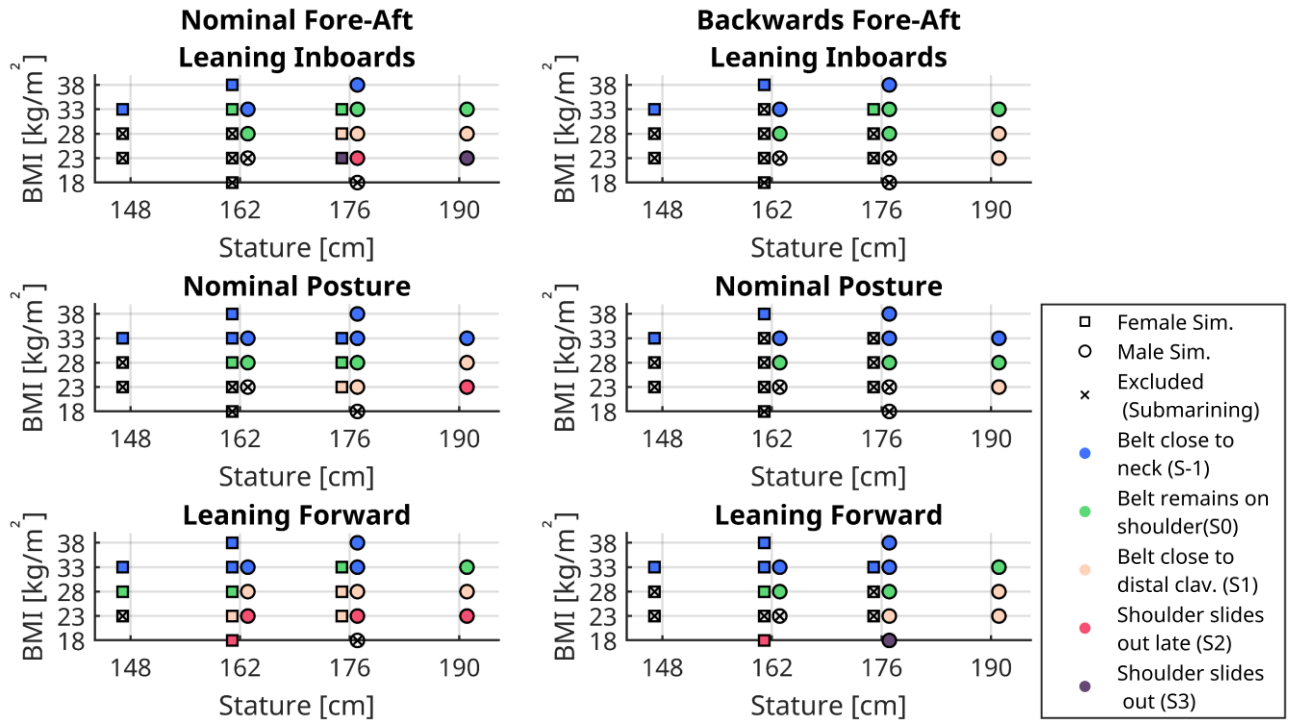

Fig. E.2. Shoulder belt to clavicle interaction classification with the ISBP belt configuration.

Appendix F

Shoulder Belt to Clavicle Interaction Classification, Far-Side Impacts

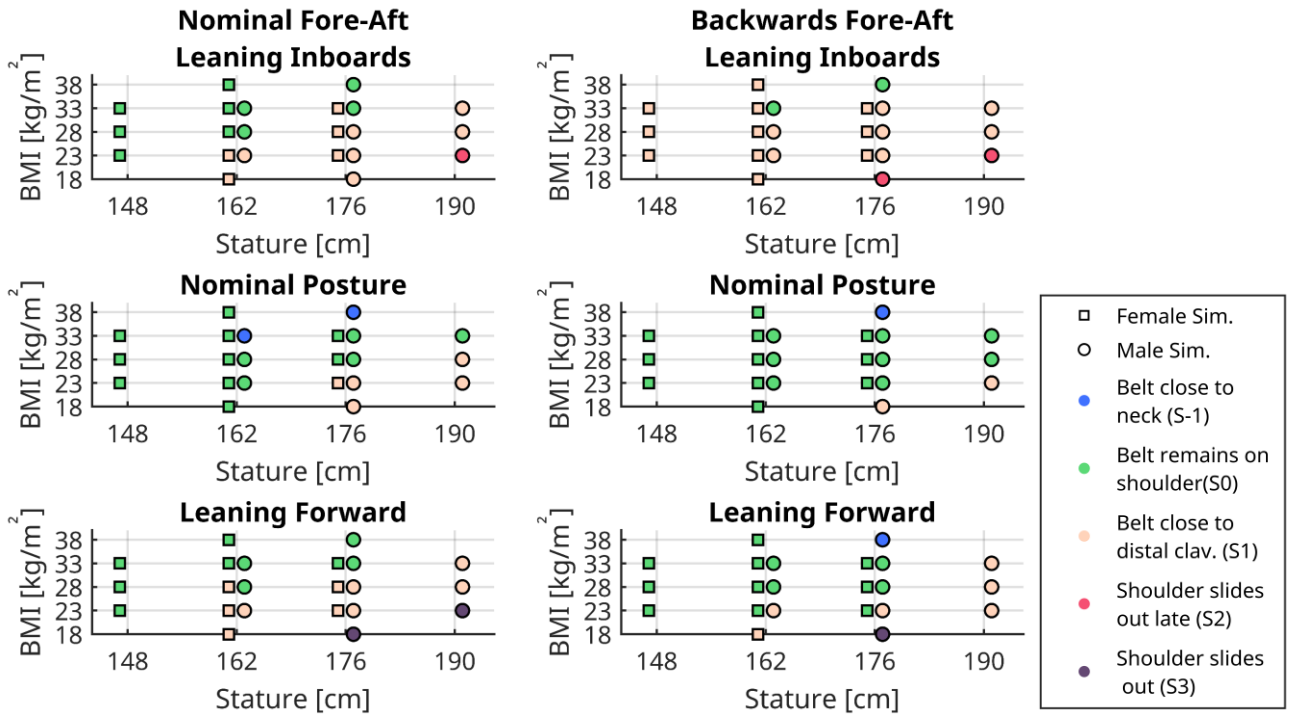

Fig. F.1. Shoulder belt to clavicle interaction classification with the traditional belt configuration.

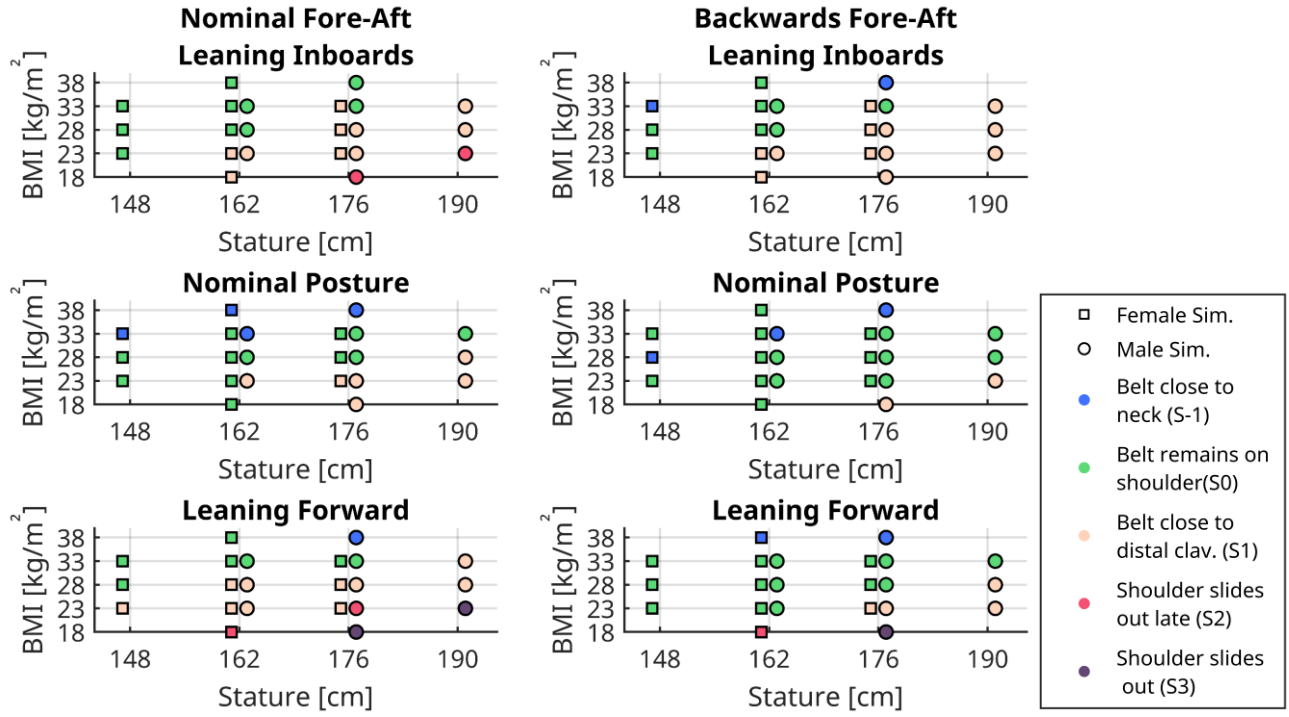

Fig. F.2. Shoulder belt to clavicle interaction classification with the ISBP belt configuration.